SANDIA REPORT
SAND2010–7583
Unlimited Release
Printed October 2010

SPR Salt Wall Leaching Experiments in Lab-Scale Vessel – Data Report

Timothy J. O'Hern, Joel D. Hartenberger, and Stephen W. Webb

Prepared by
Sandia National Laboratories
Albuquerque, New Mexico 87185 and Livermore, California 94550

Sandia National Laboratories is a multi-program laboratory managed and operated by Sandia Corporation, a wholly owned subsidiary of Lockheed Martin Corporation, for the U.S. Department of Energy's National Nuclear Security Administration under contract DE-AC04-94AL85000

Approved for public release; further dissemination unlimited.

Sandia National Laboratories

Issued by Sandia National Laboratories, operated for the United States Department of Energy by Sandia Corporation.

NOTICE: This report was prepared as an account of work sponsored by an agency of the United States Government. Neither the United States Government, nor any agency thereof, nor any of their employees, nor any of their contractors, subcontractors, or their employees, make any warranty, express or implied, or assume any legal liability or responsibility for the accuracy, completeness, or usefulness of any information, apparatus, product, or process disclosed, or represent that its use would not infringe privately owned rights. Reference herein to any specific commercial product, process, or service by trade name, trademark, manufacturer, or otherwise, does not necessarily constitute or imply its endorsement, recommendation, or favoring by the United States Government, any agency thereof, or any of their contractors or subcontractors. The views and opinions expressed herein do not necessarily state or reflect those of the United States Government, any agency thereof, or any of their contractors.

Printed in the United States of America. This report has been reproduced directly from the best available copy.

Available to DOE and DOE contractors from
U.S. Department of Energy
Office of Scientific and Technical Information
P.O. Box 62
Oak Ridge, TN 37831

Telephone: (865)576-8401
Facsimile: (865)576-5728
E-Mail: reports@adonis.osti.gov
Online ordering: http://www.doe.gov/bridge

Available to the public from
U.S. Department of Commerce
National Technical Information Service
5285 Port Royal Rd
Springfield, VA 22161

Telephone: (800)553-6847
Facsimile: (703)605-6900
E-Mail: orders@ntis.fedworld.gov
Online ordering: http://www.ntis.gov/help/ordermethods.asp?loc=7-4-0#online

SAND2010-7583
Unlimited Release
Printed October 2010

SPR Salt Wall Leaching Experiments in Lab-Scale Vessel – Data Report

Timothy J. O'Hern and Joel D. Hartenberger
Engineering Sciences Center
Sandia National Laboratories
P.O. Box 5800
Albuquerque, NM 87185-0834

Stephen W. Webb
Energy, Resource, and Systems Analysis Center
Sandia National Laboratories
P.O. Box 5800
Albuquerque, NM 87185-0706

Abstract

During cavern leaching in the Strategic Petroleum Reserve (SPR), injected raw water mixes with resident brine and eventually interacts with the cavern salt walls. This report provides a record of data acquired during a series of experiments designed to measure the leaching rate of salt walls in a lab-scale simulated cavern, as well as discussion of the data. These results should be of value to validate computational fluid dynamics (CFD) models used to simulate leaching applications. Three experiments were run in the transparent 89-cm (35-inch) ID diameter vessel previously used for several related projects. Diagnostics included tracking the salt wall dissolution rate using ultrasonics, an underwater camera to view pre-installed markers, and pre- and post-test weighing and measuring salt blocks that comprise the walls. In addition, profiles of the local brine/water conductivity and temperature were acquired at three locations by traversing conductivity probes to map out the mixing of injected raw water with the surrounding brine.

The data are generally as expected, with stronger dissolution when the salt walls were exposed to water with lower salt saturation, and overall reasonable wall shape profiles. However, there are significant block-to-block variations, even between neighboring salt blocks, so the averaged data are considered more useful for model validation. The remedial leach tests clearly showed that less mixing and longer exposure time to unsaturated water led to higher levels of salt wall dissolution. The data for all three tests showed a dividing line between upper and lower regions, roughly above and below the fresh water injection point, with higher salt wall dissolution in all cases, and stronger (for remedial leach cases) or weaker (for standard leach configuration) concentration gradients above the dividing line.

Acknowledgment

Professor Darryl James of Texas Tech University was instrumental in the experiment planning stages, as well as in calibrating the ultrasonic transducers, storing data from the transducers, and running the experiments. Shane Adee, SNL Dept. 6774, did most of the mechanical setup and assisted greatly in long hours running the tests. Chuck Hanks, SNL Dept. 1534, wrote the LabVIEW traverse control program for the conductivity/temperature probes. Tikia Allen, a student intern from Tuskegee University, helped with conductivity probe calibration procedures and preliminary investigations into diagnostic techniques.

Sandia is a multiprogram laboratory operated by Sandia Corporation, a Lockheed Martin Company, for the United States Department of Energy's National Nuclear Security Administration under Contract DE-AC04-94AL85000.

Table of Contents

1. Introduction **11**
2. Experimental Facility **12**
3. Diagnostics and Data **17**
4. Discussion **46**
5. Conclusions **47**
Appendix A – Ultrasonic Data for Test SL1 ..... **49**
Appendix B – Ultrasonic Data for Test RL2 ..... **53**
6. References **57**
7. Distribution **58**

List of Figures

Figure 2.1. Top view of experimental setup with an equivalent 0.242-inch (0.6 cm) ID injection tube (1:40 scale of SPR cavern based on injection tube). Acrylic vessel has 35-inch (89-cm) inner diameter. Diameter inside salt walls is 24.5 ± 0.5 inches (62.2 ± 1.3 cm). 12
Figure 2.2. Experimental setup for the two types of experiments. (a) Standard leaching test with 7 rows of salt blocks, separate but coaxial injection and withdrawal locations (SL1). (b) Remedial leach setup with 4 rows of salt blocks, injection and withdrawal through common tube (RL1), injection though upper and withdrawal through lower (RL2). 13
Figure 2.3. Tubing used for injection and withdrawal, end view (left), side view (right). The pumps were connected to the tubing assembly through a Swagelok T at the top. The 0.049 in^2 injection area yields an equivalent injection diameter of 0.25 in (0.63 cm)..... 14
Figure 2.4. Water level vs. time for the two remedial leach tests. (a) Test RL1 in which withdrawal was initiated as soon as injection was stopped. (b) Test RL2 in which there was a one hour settling period prior to initiating withdrawal. Also shown in these plots are the locations of the conductivity/temperature probes throughout the test period..... 16
Figure 3.1. Withdrawal line density log for the standard leach test (SL1). Error bars represent uncertainty of one additional droplet (0.05 g) of sample pipetted into the weigh boat..... 17
Figure 3.2. Withdrawal line density log for the remedial leach tests (RL1 and RL2). Error bars represent uncertainty of one additional droplet (0.05 g) of sample pipetted into the weigh boat..... 18
Figure 3.3. Preliminary test of ultrasonic technique to measure changes in salt block thickness as it dissolved. This test was run at the equipment manufacturer's site (Sonatest Inc., San Antonio, TX). 19
Figure 3.4. Location of ultrasonic transducers relative to face of salt block. Face view (left), top view (right). 20
Figure 3.5. Ultrasonic measurement of salt block dissolution during Test RL1. a) Raw data, b) Large jumps removed. 21
Figure 3.6. Representative "good" data showing measured ultrasonic spectrum from Transducer 7, Test SL1, background before test started. "Distance" on the x-axis is the distance from the transducer to the face of the salt block, which is converted to dissolved depth into the salt blocks by subtracting the initial (background) value. The operator must choose the location and height of the gate, whose choice impacts the results. As indicated in the legend, different results are determined depending on the data analysis used. Not all of the measured spectra are as clean as this one. 22
Figure 3.7. Representative "poor" data showing measured ultrasonic spectrum. In this case it is not clear which peak corresponds to the strongest reflected signal. Data like this one were not included in the plots (Figure 3.8 and Appendices). 22
Figure 3.8. Representative data showing ultrasonic measurement of salt block dissolution during leaching test. This is for the top row of blocks for the full leach configuration. Error bars indicate ±5%..... 23

Figure 3.9. Salt block from top row of blocks during Test RL2. This shows the unwetted portion of the block whose weight is estimated and compensated for in the data shown in Table 3.2. 26
Figure 3.10. Row-averaged mass loss as a function of height in the tank (plotted at center of each row of salt blocks). Data are from Table 3.2. Note that injection and withdrawal depths are only valid for test SL1. 27
Figure 3.11. Shape of the upper five rows of salt blocks removed from tank following Test SL1. The bottom two rows of salt blocks were undissolved (several weights checked to verify this) and were reused in the next test (RL2). See Table 3.2 for the pre- and post-test block weights. 29
Figure 3.12. Shape of the four rows of salt blocks removed from tank following first remedial leach test (RL1). See Table 3.2 for the pre- and post-test block weights. 30
Figure 3.13. Shape of the four rows of salt blocks removed from tank following second remedial leach test (RL2). See Table 3.2 for the pre- and post-test block weights. There is much more dissolution in the upper rows for this test than in the Test RL1. 31
Figure 3.14. Microscale Conductivity/Temperature Probe from Precision Measurement Engineering. 32
Figure 3.15. Probe locations in tank. Probe numbers (186, 193, 195) correspond to preamplifier/excitation electronics. 33
Figure 3.16. Probe locations in tank during Test SL1. 33
Figure 3.17. Temperature calibration data for all three MSCTI probes, performed 1/26/09 prior to testing. Temperature calibration is quite stable and only needs an occasional check. The points in this figure are the measured values and the dashed lines are the curve fits used in the temperature data conversion. 34
Figure 3.18. Conductivity calibration data for all three MSCTI probes performed immediately prior to Test SL1, before installing probes in tank. The polynomial fits are the calibration curves used to convert measured voltages to NaCl saturation level. 35
Figure 3.19. Conductivity calibration data for all three MSCTI probes performed immediately prior to Test RL1, before installing probes in tank. The polynomial fits are the calibration curves used to convert measured voltages to NaCl saturation level. 35
Figure 3.20. Conductivity calibration data for all three MSCTI probes performed immediately prior to Test RL2, before installing probes in tank. The polynomial fits are the calibration curves used to convert measured voltages to NaCl saturation level. 36
Figure 3.21. Temperature profiles: Probe 195, Test SL1 (probes 186 and 193 very similar for this test). The legend shows depth in tank at which data were taken, measured up from the tank floor. The upper dashed line indicates the depth of the injection line and the lower dashed line the depth of the withdrawal line. 38
Figure 3.22. Temperature profiles: Probe 186, Test RL1 (probes 193 and 195 very similar for this test). The legend shows times at which data were taken. Flow was reversed from injection to withdrawal at 12:45 (2.5 hours after start of injection). 38
Figure 3.23. Temperature profiles: Probe 193, Test RL2 (probes 186 and 195 very similar for this test). The legend shows depth in tank at which data were taken,

measured up from the tank floor. Injection stopped at 11:53, withdrawal started at 12:55. 39
Figure 3.24. Concentration profiles: Probe 186, Test SL1. Legend shows time data were taken. Conductivity data have been corrected for temperature changes during test and between calibration and test. 39
Figure 3.25. Concentration profiles: Probe 193, Test SL1. Legend shows time data were taken. Conductivity data have been corrected for temperature changes during test and between calibration and test. 40
Figure 3.26. Concentration profiles: Probe 195, Test SL1. Legend shows time data were taken. Conductivity data have been corrected for temperature changes during test and between calibration and test. 40
Figure 3.27. Concentration profiles: Probe 186, Test RL1. Legend shows time data were taken. Flow was reversed from injection to withdrawal at 12:45 (2.5 hours after start of injection). The dashed line indicates the depth of the injection/withdrawal line. Conductivity data have been corrected for temperature changes during test and between calibration and test. 41
Figure 3.28. Concentration profiles: Probe 193, Test RL1. Legend shows time data were taken. Flow was reversed from injection to withdrawal at 12:45 (2.5 hours after start of injection). Conductivity data have been corrected for temperature changes during test and between calibration and test. 41
Figure 3.29. Concentration profiles: Probe 195, Test RL1. Legend shows time data were taken. Flow was reversed from injection to withdrawal at 12:45 (2.5 hours after start of injection). Conductivity data have been corrected for temperature changes during test and between calibration and test. 42
Figure 3.30. Concentration profiles: Probe 186, Test RL2. Legend shows time data were taken. Injection stopped at 11:53, withdrawal started at 12:55. The dashed line indicates the depth of the withdrawal line. Conductivity data have been corrected for temperature changes during test and between calibration and test. 42
Figure 3.31. Concentration profiles: Probe 193, Test RL2. Legend shows time data were taken. Injection stopped at 11:53, withdrawal started at 12:55. Conductivity data have been corrected for temperature changes during test and between calibration and test. 43
Figure 3.32. Concentration profiles: Probe 195, Test RL2. Legend shows time data were taken. Injection stopped at 11:53, withdrawal started at 12:55. Conductivity data have been corrected for temperature changes during test and between calibration and test. 43
Figure 3.33. Photo showing salt walls and tank floor after test SL1. 44
Figure A.1. Ultrasonic data for ultrasonic transducer 1, Test SL1. 49
Figure A.2. Ultrasonic data for ultrasonic transducer 2, Test SL1. 49
Figure A.3. Ultrasonic data for ultrasonic transducer 3, Test SL1. This plot shows the type of ultrasonic spectra that yielded useful data (right) and data that were not used (left). In this case, the true peak was cut off by the settings needed to eliminate noise sufficiently to acquire a stable signal. Histogram data like these exists for every point in the dissolution vs. time plots but was not all included in this report. 50
Figure A.4. Ultrasonic data for ultrasonic transducer 4, Test SL1. 51
Figure A.5. Ultrasonic data for ultrasonic transducer 5, Test SL1. 51

Figure A.6. Ultrasonic data for ultrasonic transducer 6, Test SL1. 52
Figure A.7. Ultrasonic data for ultrasonic transducer 7, Test SL1. 52
Figure B. 1. Ultrasonic data for ultrasonic transducer 1, Test RL1 53
Figure B. 2. Ultrasonic data for ultrasonic transducer 2, Test RL1 53
Figure B. 3. Ultrasonic data for ultrasonic transducer 3, Test RL1 54
Figure B. 4. Ultrasonic data for ultrasonic transducer 4, Test RL1 54
Figure B. 5. Ultrasonic data for ultrasonic transducer 5, Test RL1 55
Figure B. 6. Ultrasonic data for ultrasonic transducer 6, Test RL1 55
Figure B. 7. Ultrasonic data for ultrasonic transducer 7, Test RL1 56

List of Tables

Table 2.1. Test conditions. 14
Table 3.1. Ultrasonic transducer locations. The blocks were stacked in rows of 12 starting with the North column so blocks 1, 13, 25, 37, 49, and 61 were in this column; with the numbering starting on the bottom row (see Figures 2.1 and 2.2). 20
Table 3.2. Pre- and post-test block weights. Note that the bottom two rows of blocks from Test SL1 were undissolved and therefore not removed and weighed (except for a few spot checks not listed in this table), and were reused for the Test RL2. The red entries indicate mass gain which is thought to be due to accuracy of the Taylor TE-400 digital scale used (±0.5 lb). 26
Table 3.3. Initial and final salt mass in the system for each test. Uncertainties in the estimated liquid values are due to uncertainties in the exact brine volume (based on wall thicknesses before and after dissolution) and in the final brine concentration in the tank post-test. 44

1. Introduction

During cavern leaching in the Strategic Petroleum Reserve (SPR), injected raw water mixes with resident brine and eventually interacts with the cavern salt walls. Whenever less-than-saturated brine contacts the salt walls, dissolution will occur, leading to leaching of the salt walls. This report provides a record of data acquired during a series of experiments designed to measure the leaching rate of salt walls in a lab-scale simulated cavern, as well as discussion of the data. These results should be of value to validate computational fluid dynamics (CFD) models used to simulate leaching applications. Three experiments were performed in February 2009 in the transparent 89-cm (35-inch) ID diameter vessel previously used for several related projects. Diagnostics included tracking the salt wall dissolution rate using ultrasonics, an underwater camera to view pre-installed markers, and pre- and post-test weighing and measuring salt blocks that comprise the walls. In addition, profiles of the local brine/water conductivity and temperature were acquired at three locations by traversing conductivity probes to map out the mixing of injected raw water with the surrounding brine, and samples were taken from the withdrawal line and their density measured.

Detailed leaching data including the spatial distribution are needed to validate CFD models for cavern leaching. As discussed by Webb (2008), previous data-model comparisons for leaching in the tank used in these experiments only considered the brine concentration values in the tank, not the actual wall dissolution data. The present experiments provide spatial dissolution information that will be used to further evaluate mechanistic CFD leaching models.

Experiment completion and representative data were presented in O'Hern and Webb (2009). Further analysis, plots, and discussion of the salt wall leaching data are presented in this report.

2. Experimental Facility

The experiments performed here, described in O'Hern and Webb (2008, 2009), were performed in a large transparent vessel configured for use as a scale model SPR cavern. Two types of experiments were performed, a standard leaching (SL) configuration and one more representative of a remedial leach (RL) situation. Each will be described in more detail below. In both cases, the flow rate was determined by scaling to match the ratio of buoyancy to momentum forces between the experiment and the SPR cavern.

Test Apparatus

Figures 2.1 and 2.2 show the experimental setup that uses the tank and injection/withdrawal system and configurations described in O'Hern and Webb (2008, 2009). As in prior tank tests, the cavern-to-laboratory flow rate scaling was determined by keeping the Froude number *Fr*, or ratio of momentum to buoyant force, equal between the nominal cavern conditions and the laboratory setup (Turner, 1979). The current laboratory experiments were run at a nominal scaled flowrate equivalent to the nominal SPR cavern value of 100,000 barrels per day, which yields a laboratory flow rate of 0.3 GPM. Salt blocks were machined to a wedge shape as shown in Figure 2.1, so that when fitted together the salt block assembly formed a fairly continuous salt wall.

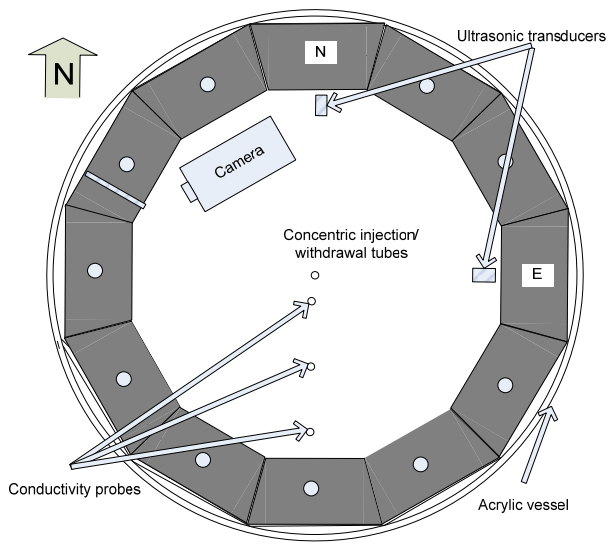

Figure 2.1. Top view of experimental setup with an equivalent 0.242-inch (0.6 cm) ID injection tube (1:40 scale of SPR cavern based on injection tube). Acrylic vessel has 35-inch (89-cm) inner diameter. Diameter inside salt walls is 24.5 ± 0.5 inches (62.2 ± 1.3 cm).

For all tests, salt walls were fabricated from salt blocks machined from commercial salt licks obtained at a local feed store. The nominal dimensions of the original salt blocks are roughly 9 × 9 × 10.5 inches (23 × 23 × 27 cm). These blocks were machined by cutting them in half, then wedging the walls to form the trapezoid shape shown in Figure 2.1, nominally 4.5 inches (11.4 cm) deep, 10.5 inches (26.7 cm) high, 6.5 inch (16.5 cm) front face, and 8.5 inch (21.6 cm) back face (all dimensions ± 0.5 inch (1.3 cm) for raw material and machining tolerances). In order to prevent dissolution of the back sides of the blocks (facing away from the center of the tank but still underwater), the backs of the blocks were coated with Liquid Rock 2-part epoxy (Demand Products, Inc., Alpharetta, GA). When installed in the tank, the salt blocks in each column were connected together using ½" (1.3 cm) diameter phenolic rods placed into pre-drilled through holes to keep them from falling. At the top of

each column the phenolic rods were strapped together and tightened until the walls were fairly straight, sturdy, and well-sealed. The average inner diameter of the salt walls in each test was 24.5 ± 0.5 inches (62.2 ± 1.3 cm). An additional 50 lb (23 kg) bag of salt was added as a loose salt floor prior to each test.

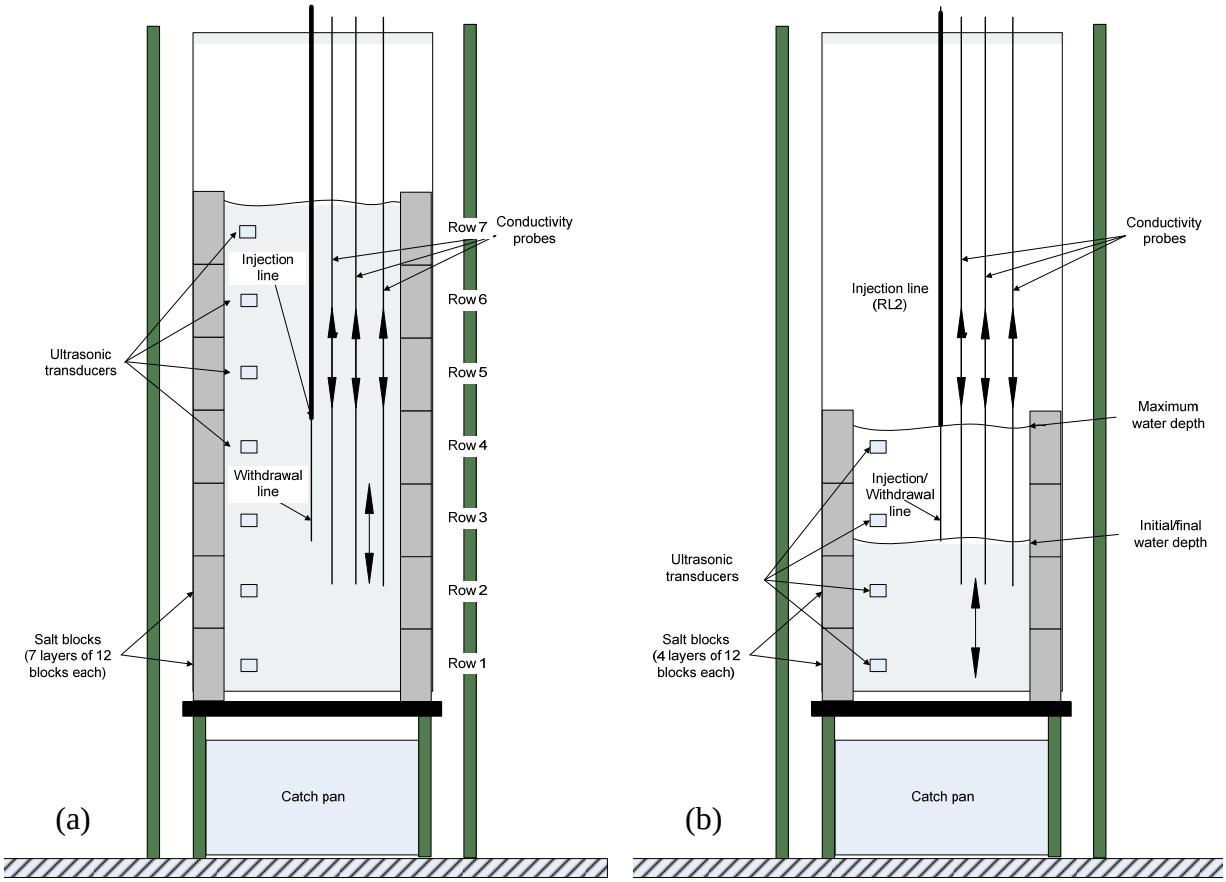

Figure 2.2. Experimental setup for the two types of experiments. (a) Standard leaching test with 7 rows of salt blocks, separate but coaxial injection and withdrawal locations (SL1). (b) Remedial leach setup with 4 rows of salt blocks, injection and withdrawal through common tube (RL1), injection though upper and withdrawal through lower (RL2).

For all tests, the salt-lined tank was filled with a premixed saturated NaCl solution (density checked to be 1.2 g/cc) prior to the test. An additional 50 lb (23 kg) loose salt was added to form a salt floor in the tank. The fresh water to be injected was placed in 55 gallon plastic tanks alongside the large tank and left for at least 24 hours to allow the temperature to stabilize at room temperature (20.5 ± 1°C). Water injection and withdrawal were done using Barnant "Vera" model peristaltic pumps. The injection and withdrawal plumbing is shown in Figure 2.3. The pumps were connected to the injection/withdrawal tubes through 1/4" ID, 3/8" OD Tygon© silicone tubing. The experimental configurations are listed in Table 2.1 and discussed below:

No roof protection oil was used in the present tests, but instead air was present above the water. Therefore both SL and RL lab test configurations utilized air as the inert roof protection fluid instead of the oil found in SPR caverns. If there is any effect due to this setup, it is more likely to appear in the RL case with a moving interface. The oil is more likely to wet the salt walls than the air and thus delay the exposure of the salt to the unsaturated brine, but the extent to which this affects leaching rate in a real system is unknown.

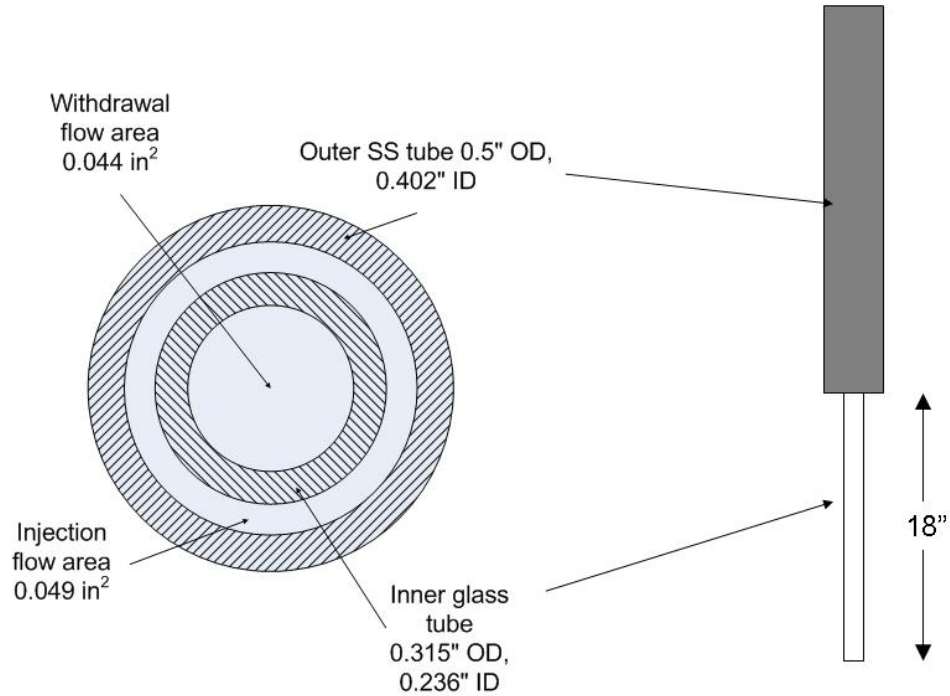

Figure 2.3. Tubing used for injection and withdrawal, end view (left), side view (right). The pumps were connected to the tubing assembly through a Swagelok T at the top. The 0.049 in^2 injection area yields an equivalent injection diameter of 0.25 in (0.63 cm).

Test	**SL1**	**RL1**	**RL2**
Configuration	Standard	Remedial	Remedial with one hour static
Date	2/16/09	2/12/09	2/18/09
Height of salt walls	74 ± 2 inch (7 rows) (188 ± 5.1 cm)	42 ± 1 inch (4 rows) (107 ± 2.5 cm)	42 ± 1 inch (4 rows) (107 ± 2.5 cm)
Diameter of chamber inside salt walls	24.5 ± 0.5 inches (62.2 ± 1.3 cm)	24.5 ± 0.5 inches (62.2 ± 1.3 cm)	24.5 ± 0.5 inches (62.2 ± 1.3 cm)
Injection flowrate (mean ± standard deviation)	0.30 ± 0.03 GPM	0.30 ± 0.01 GPM	0.30 ± 0.02 GPM
Withdrawal flowrate (mean ± standard deviation)	0.29 ± 0.04 GPM	0.33 ± 0.01 GPM	0.30 ± 0.01 GPM
Run time (hours)	9:00	4:57	6:10
Comments			Injection at water-air interface

Table 2.1. Test conditions.

Standard leaching (SL) Test

The standard leaching configuration used to construct an underground storage cavern requires a raw water injection string, a brine withdrawal string, and a roof protection fluid that floats on top of the brine to prevent leaching above a prescribed depth. For typical SPR applications there are actually two standard leach configurations used to construct a cavern. First, a direct leaching configuration is used in which the injection string is positioned deeper than the withdrawal string to promote leaching in the deepest part of the cavern. Next, a reverse leaching configuration is used where the injection string is positioned above the withdrawal string to promote leaching in the upper portions of the cavern. The specific configuration simulated is this laboratory standard leach test is the reverse configuration in which the raw water is injected above the withdrawal string. The level of roof protection fluid, which is air in this case, remains static during the test.

In the lab SL test, shown in Figure 2.2(a), the salt walls were seven layers high (approximately 74 inch (188 cm) average wall height). The tank was initially filled with saturated NaCl brine to a fill height of 71.5 inches (182 cm), near the top of the shortest column of salt blocks. Fresh water injection was made at 30.5 inches (77.5 cm) below the surface, and withdrawal was made through a coaxial withdrawal tube 18 inches (45.7 cm) below injection (see Figures 2.2 and 2.3), which scales to a cavern equivalent of 59 ft (18 m) below the injection location, through geometric scaling based on the injection tube equivalent diameter. The injection and withdrawal flow rates were matched to maintain a constant fill level throughout the test. This test, labeled SL1, ran for 9 hours before the upper rows of salt blocks appeared significantly dissolved. At that time the mixed water in the tank was quickly pumped out through a port in the tank base to prevent further salt wall dissolution.

Remedial leaching (RL) Tests

SPR operations use raw water (unsaturated brine) to displace oil for drawdown and delivery to offsite customers. In this configuration, raw water is injected below the oil-brine interface, and the vertical position of the roof protection fluid changes to accommodate the new volume. In this process, regions of the salt cavern walls that are exposed to raw water dissolve, which expands the cavern radius and eventually saturates the brine. The cavern is then refilled with oil, which displaces the brine. This configuration is called remedial leaching. It differs from the standard leach configuration primarily in that there is only one string to inject or withdraw water or brine. The oil-brine interface depth moves to accommodate changes in the brine volume.

In the lab RL tests, shown in Figure 2.2(b), the salt walls were four layers high (approximately 42 inch (107 cm) average wall height). The initial saturated NaCl brine fill height was approximately 23.5 inches (59.7 cm), near the bottom of the third row of blocks. Fresh water was injected, with no withdrawal, so the tank initially filled with water until it reached a predetermined depth, at which time the pump was reversed and the tank was drained at the same flowrate back to its original fill depth, at which time the remaining water was quickly drained so that the salt walls would no longer dissolve.

Two tests were run in this configuration, RL1 and RL2. In the first, RL1, injection was maintained for 2.5 hours, then the pump was reversed and withdrawal at the same rate was maintained for another 2.5 hours until the water level returned to approximately its starting level. For Test RL2, an intentional change was made in that once the maximum height was reached the tank was left undisturbed for one hour (no injection or withdrawal) before initiating the 2.5 hour withdrawal. The water level changes during these two tests are plotted in Figure 2.4. An additional unintentional difference in Test RL2 was that the fresh water was inadvertently injected through the upper stainless steel injection tube approximately 18 inches (45.7 cm) above the initial brine-air interface, rather than through the lower glass withdrawal tube initially at the brine-air interface. This was not detected because the water flowed down around the inner glass tube and into the tank without splashing, and was only detected

when it was time to begin withdrawal, at which time the tubing was fixed so that withdrawal was through the correct (lower depth) tube (see Figure 2.2 (right)). Because of this plumbing problem, as the water level in this test rose, mixing was minimized as the less dense fresh water was added on top of the denser brine below. The effect of this configuration will be discussed with the data below.

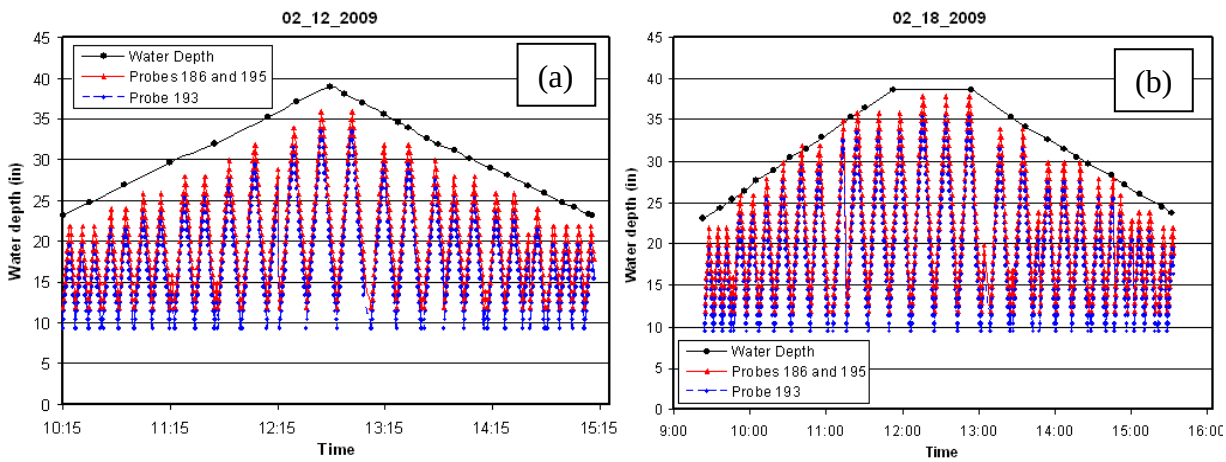

Figure 2.4. Water level vs. time for the two remedial leach tests. (a) Test RL1 in which withdrawal was initiated as soon as injection was stopped. (b) Test RL2 in which there was a one hour settling period prior to initiating withdrawal. Also shown in these plots are the locations of the conductivity/temperature probes throughout the test period.

3. Diagnostics and Data

Standard measurements included monitoring the flow rates in and out of the tank, and the temperature in the room. The flow rates, measured by tracking the water levels in the injection and withdrawal tanks, were measured approximately every 15 minutes and the values were given in Table 2.1 The room and injection tank temperatures were always 20.5 ± 1 °C for all three tests. More detailed diagnostic techniques are discussed individually below, along with data sets and plots.

Density sampling

30-ml samples of the withdrawal water were grabbed approximately every 15 minutes and stored in sealed glass jars for off-line density measurements. The densities were measured using a Mettler-Toledo PB4002-S/FACT scale (0.01 g repeatability) by carefully pipetting a 10-ml sample into a weigh boat. Figures 3.1 and 3.2 show the withdrawal line density samples for the standard and remedial tests, respectively. Note that for Test SL1 (Figure 3.1) the initial density is that of water saturated with the salt block material.

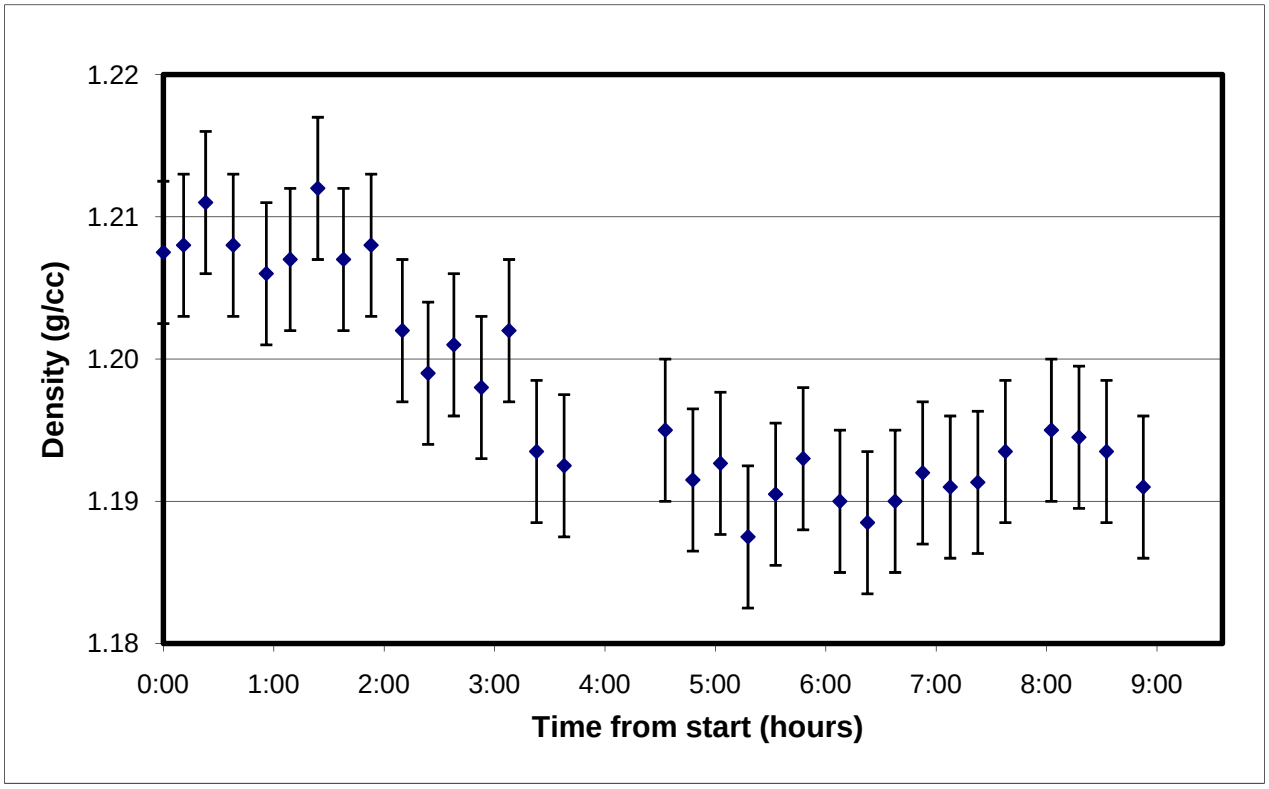

Figure 3.1. Withdrawal line density log for the standard leach test (SL1). Error bars represent uncertainty of one additional droplet (0.05 g) of sample pipetted into the weigh boat.

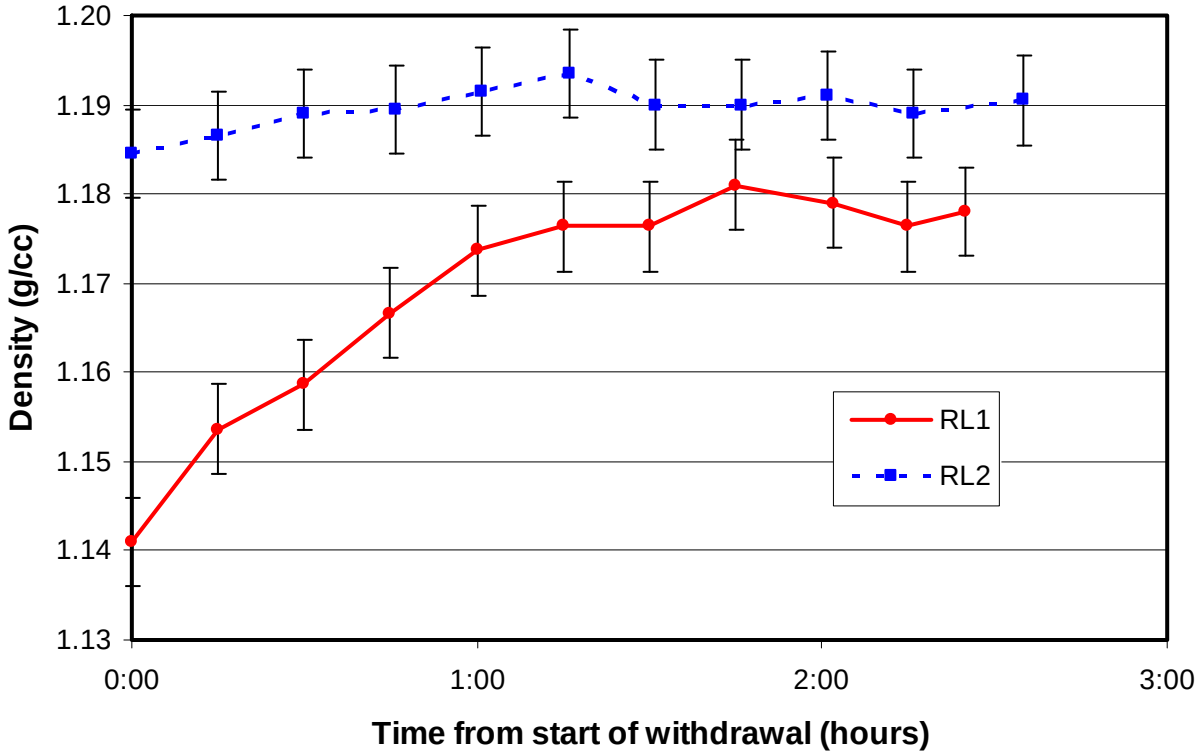

Figure 3.2. Withdrawal line density log for the remedial leach tests (RL1 and RL2). Error bars represent uncertainty of one additional droplet (0.05 g) of sample pipetted into the weigh boat.

Interpretation of Figures 3.1 and 3.2 is complicated by the combined effects of mixing between the fresh water and brine and salt wall dissolution.

Figure 3.1 shows that for Test SL1 (continuous injection and withdrawal at the same flow rate) that the mixed water had not reached the withdrawal tube for the first two hours of the run. Once the mixed water reached the withdrawal tube the density continuously decreased for 4 hours until it seemed to stabilize around a slightly lower value of 1.19 g/cc.

Figure 3.2 shows the densities measured in the withdrawal tube for the remedial leach cases. For the first half of each of these tests fresh water was injected with no withdrawal, so no densities were measured and the water level rose above the end of the withdrawal tube. The data start at the beginning of the withdrawal period. The Test RL1 densities show a continuous increase in density in the water removed from the tank. The fresh water (1.00 g/cc) was injected through the same tube as the withdrawal. Figure 3.2 shows that the withdrawn water from the RL2 remedial leach configuration was always near saturation. This was due to density stratification caused by the plumbing problem in Test RL2 that sent water through the upper injection tube (as discussed and shown in Section 2), and the hour of static dissolution between injection and withdrawal which allowed the water to dissolve enough salt to be nearly saturated at the withdrawal location.

Ultrasonics

Piezoelectric ultrasonic transducers were set up to emit a burst of high frequency sound waves directed at the surface of a nearby salt block. Some of the energy was reflected by the surface and received at the transducer. The distance between the transducer and the face of the block was computed from the time of flight. Ideally, as the salt dissolves the increasing distance between the transducer and the salt block will show up in an increased time of flight.

Seven of the 1-MHz transducers tested at Sonatest (http://www.sonatest.com/, see O'Hern and Webb, 2008) were calibrated and used in these tests. The ultrasonic control unit was a Sonatest Masterscan 380, generously loaned by Sonatest for two weeks during testing. There is an issue in that the salt does not dissolve uniformly but in an uneven manner as seen in Figure 3.3, so the ultrasound reflection weakens as the block dissolves. However, if the transducer is initially positioned close to the block the signal remains strong enough over a significant portion of the salt block dissolution. An additional advantage of positioning the transducer close to the block is that the ultrasound path length through the water is minimized. As discussed in Al-Nassar et al. (2006), the sound speed is a function of the local salt concentration. Since the salt concentration in the gap between each transducer and the corresponding salt block could not be monitored during the tests, it was assumed to be saturated. This is expected to lead to experimental uncertainty on the order of 10%. The sound speed in pure water is on the order of 20% lower than that in saturated brine (depending on temperature), and the water in the vicinity of the transducers is expected to be at most about 50% saturated.

Seven transducers were mounted in the tank for these tests at the locations listed in Table 3.1. The transducers were positioned about halfway up each block and about one-quarter of the way across each block (see Figure 3.4) to measure dissolution in a part of the salt block that did not include the center connecting rod through-hole. For the standard leach test all seven transducers were mounted along a single column of blocks (see Table 3.1) and were submerged throughout the entire test. For the remedial leach tests only the lowest transducers were always submerged and taking data and the upper ones were only powered on and operated when the water level was high enough to submerge them.

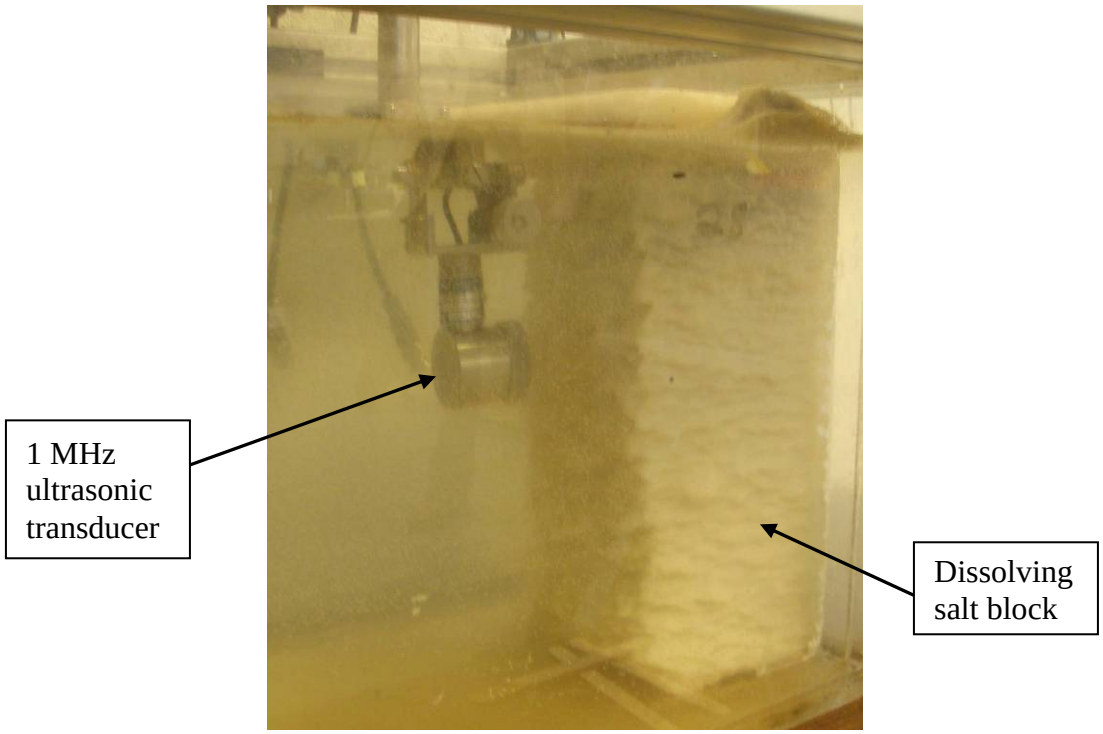

Figure 3.3. Preliminary test of ultrasonic technique to measure changes in salt block thickness as it dissolved. This test was run at the equipment manufacturer's site (Sonatest Inc., San Antonio, TX).

	Transducer location (Column (see Figure 2.1), Row, block #, height from tank floor (in))	
Transducer	**Test SL1**	**Tests RL1 and RL2**
1	E, 1, 10, 5.25”	E, 1, 10, 5.25”
2	E, 2, 22, 15.75”	E, 2, 22, 15.75”
3	E, 3, 34, 26.25”	E, 3, 34, 26.25”
4	E, 4, 46, 36.75”	E, 4, 46, 36.75”
5	E, 5, 58, 47.25”	N, 2, 13, 15.75”
6	E, 6, 70, 57.75”	N, 3, 25, 26.25”
7	E, 7. 82, 68.25”	N, 4, 37, 36.75”

Table 3.1. Ultrasonic transducer locations. The blocks were stacked in rows of 12 starting with the North column so blocks 1, 13, 25, 37, 49, and 61 were in this column; with the numbering starting on the bottom row (see Figures 2.1 and 2.2).

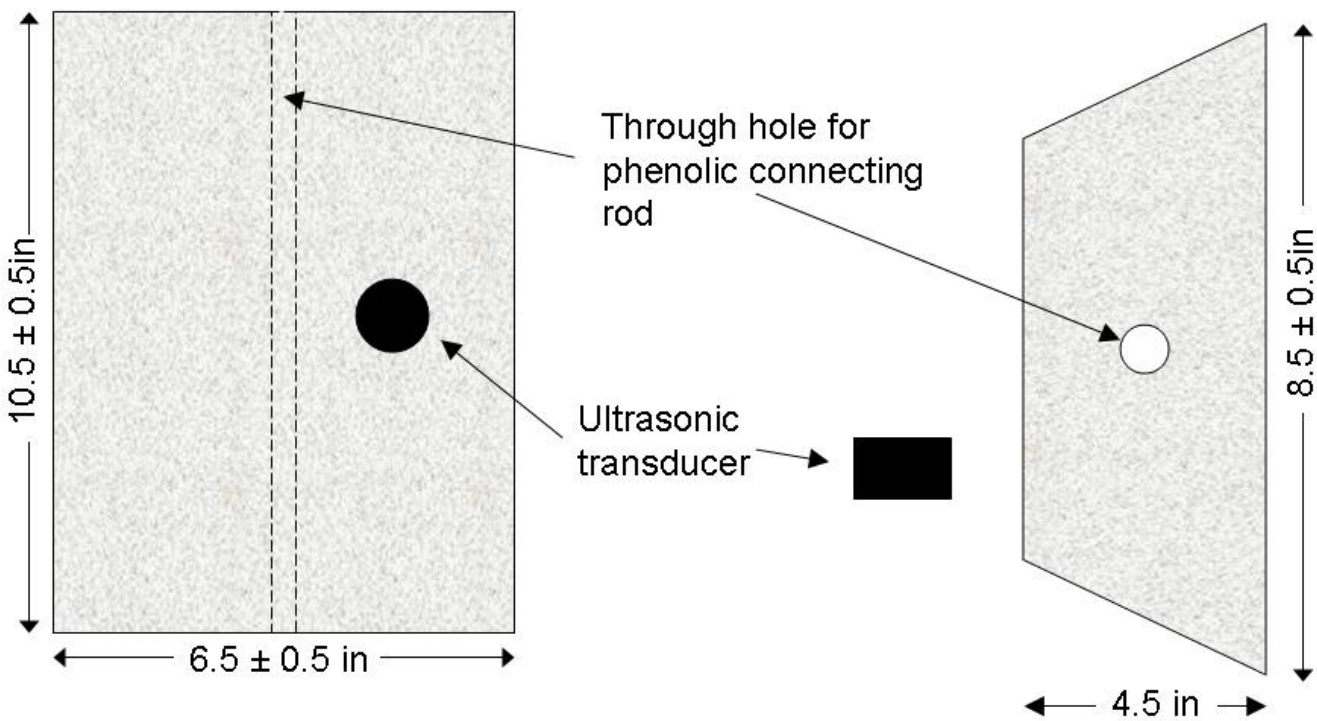

Figure 3.4. Location of ultrasonic transducers relative to face of salt block. Face view (left), top view (right).

Figure 3.5a shows the raw ultrasonic dissolution data for Test RL1. For this test, it seems reasonable to correct for the non-physical jumps in the data which were caused by movement of the structures holding the ultrasonic transducers in place. This seemed to occur whenever a manlift was moved to the top of the tank to reposition the underwater camera, take pictures, etc. Figure 3.5b shows the same data with the large jumps removed. For the subsequent tests the ultrasonic transducer supports were more rigidly fixed to the acrylic tank structure rather than to the free-standing Unistrut frame around it. In

addition, the underwater camera was no longer used since its repositioning was the major cause of problems in Test RL1.

The measured salt dissolution for each block in Tests SL1 and RL2 are shown in Appendix A and B, respectively. Some of the data indicated a negative dissolution rate (i.e., salt wall apparently thickened between measurement times). These data were not corrected but are included in the Appendices. The only data that were deleted were those in which the recorded spectrum showed improper settings for gate or range that may have cut off the correct peak. The Appendix B data in particular show negative dissolution rates. This cannot be due to changes in sound speed between fresh water and saturated NaCl brine (see Al-Nassar et al., 2006), since sound speed varies directly with salt concentration, i.e., saturated brine has the highest sound speed and fresh water the lowest. Since the ultrasonic system measures the time for an ultrasonic pulse to travel to the target and back, an uncorrected decrease in the sound speed would lead to a slower return, indicating that the target was further away than it really was. Therefore the data showing negative dissolution (salt closer to the transducer) cannot be explained by uncorrected local lower salt concentrations in the brine. The only reasonable explanation seems to be actual shifting of the salt walls as they dissolved and settled slightly during the tests.

Figures 3.6 and 3.7 show representative "good" and "poor" ultrasonic spectra measured during tests SL1 and RL2 (the software needed to store signals from the Masterscan was not received until after Test RL1 and had to be quickly installed and learned). It is clear that some of the ultrasonic signals are cleaner and simpler to analyze than others. A representative sample of measured salt dissolution for a single salt block is shown in Figure 3.8. Since only a few blocks were measured with the ultrasonic technique it is difficult to state how well the data presented are characteristic of overall wall dissolution profiles. It was observed that the blocks that were monitored seemed representative and did not have either excessive dissolution or very little dissolution, as was seen in some of the blocks (see Figures 3.11 through 3.13 and discussion there).

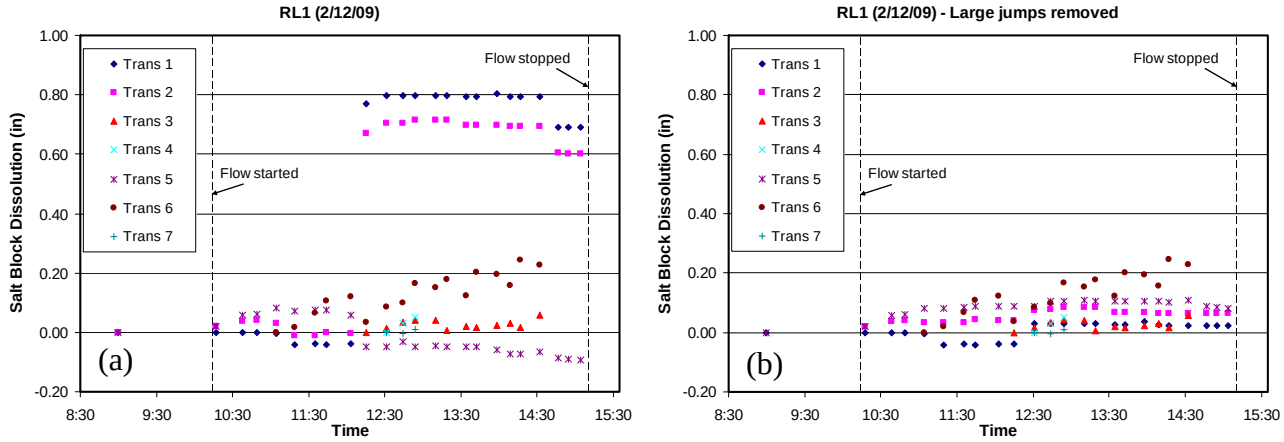

Figure 3.5. Ultrasonic measurement of salt block dissolution during Test RL1. a) Raw data, b) Large jumps removed.

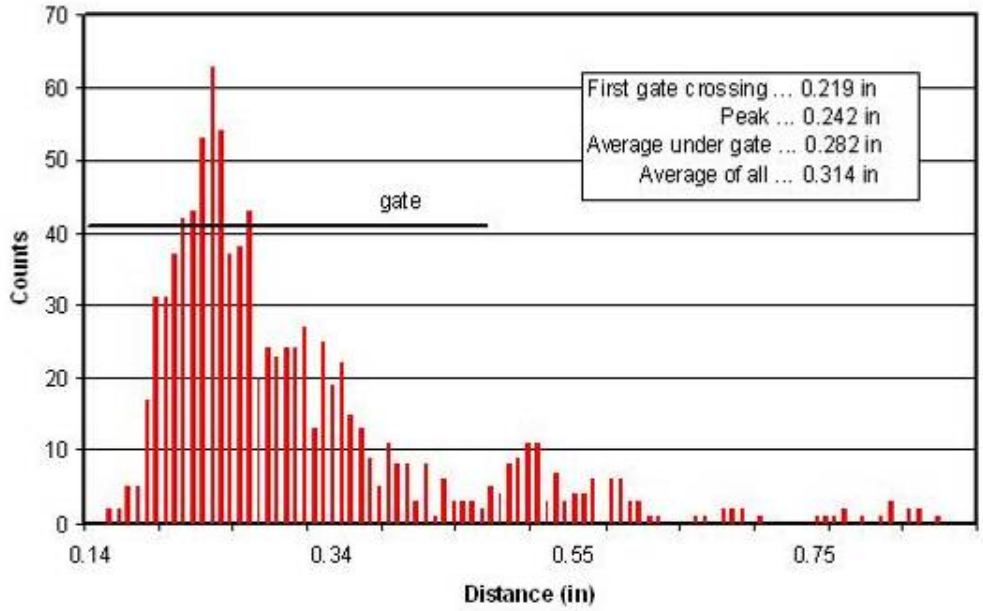

Figure 3.6. Representative "good" data showing measured ultrasonic spectrum from Transducer 7, Test SL1, background before test started. "Distance" on the x-axis is the distance from the transducer to the face of the salt block, which is converted to dissolved depth into the salt blocks by subtracting the initial (background) value. The operator must choose the location and height of the gate, whose choice impacts the results. As indicated in the legend, different results are determined depending on the data analysis used. Not all of the measured spectra are as clean as this one.

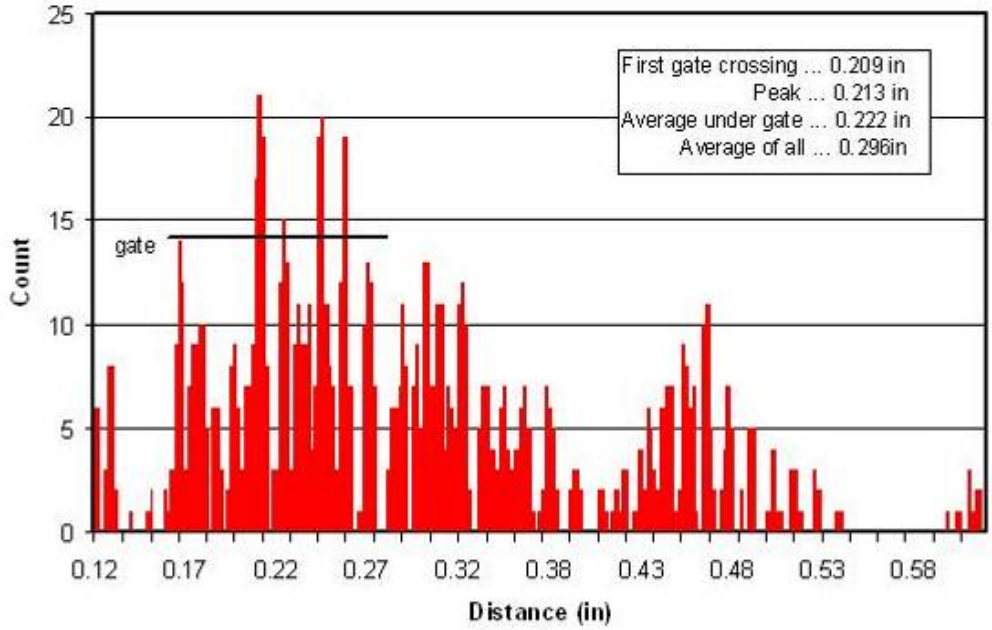

Figure 3.7. Representative "poor" data showing measured ultrasonic spectrum. In this case it is not clear which peak corresponds to the strongest reflected signal. Data like this one were not included in the plots (Figure 3.8 and Appendices).

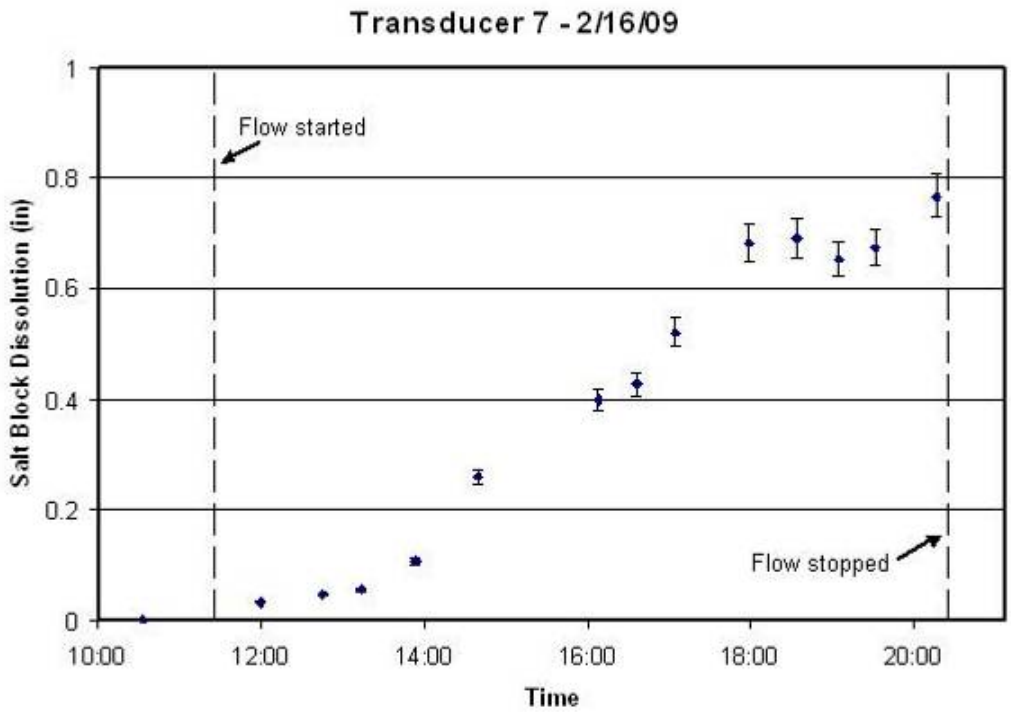

Figure 3.8. Representative data showing ultrasonic measurement of salt block dissolution during leaching test. This is for the top row of blocks for the full leach configuration. Error bars indicate ±5%.

Underwater Camera

A standard CCD camera and a light source were housed in a water-tight housing and submerged to view pre-installed markers in one column of salt blocks during the first leaching test as indicated in Figure 2.1. The camera was a Pulnix TM-745 monochrome CCD camera (768 × 493 pixel resolution, 8-bit). The digital video was recorded for later analysis, but the image quality limited the usefulness of this technique, and the camera was not used during Tests SL1 and RL2 because traversing the camera was observed to jostle the tank and supporting structure enough to affect the ultrasonic transducers during Test RL1.

Weighing/measuring

As the salt blocks comprising the salt walls were put in place each was weighed. There were 84 salt blocks for Test SL1 and 48 salt blocks for Tests RL1 and RL2. After each test, the water was drained quickly, the blocks allowed to dry, and post-test weights measured. Table 3.2 shows the pre- and post-test weights for all three tests. A Taylor TE 400 digital scale was used to make these measurements (accuracy ±0.5 lb). The weights of the top row of salt blocks (row 7 for Test SL1, row 4 for Tests RL1 and RL2) have been corrected to account for the fact that this row of blocks was only partially submerged, so a large undissolved mass remained above the water level (see Figure 3.9). The "Pre" and "Post" weight data in Table 3.2 for these blocks are estimates of the pre- and post-test weights of the wetted part of the block, subtracting the weight of the unwetted part from both the pre- and post-test measured weights.

Figure 3.10 plots the final row-averaged mass loss as a function of height in the tank for the three tests. Test SL1 had the greatest overall mass loss, as expected since fresh water was continuously added to the tank, and the test ran much longer than the remedial test cases. Test RL2 shows higher mass loss in the top row of salt blocks than Test RL1, showing that the combination of less mixing and an hour of static dissolution between injection and withdrawal were significant factors leading to increased

dissolution rates high in the tank.

Figure 3.11 is a photo showing the upper 5 rows of blocks removed from the tank following Test SL1 and Figures 3.12 and 3.13 show all 4 rows of blocks following Tests RL1 and RL2, respectively. Individual photos of each block were also recorded but not included in this report. Laying the blocks out this way allows qualitative viewing of the salt dissolution profile shown in Figure 3.10, and similar trends can be observed. One unexpected result was the large amount of block-to-block variability, even within a single row of salt blocks. For example, see Figure 3.11, block 58 (middle row of photo, left side). This block has significantly less mass loss than its neighbors at the same height. This is thought to be due more to variations in the salt block characteristics than to any flow nonuniformities, and is the reason that only row-averaged mass loss is plotted, rather than profiles of each individual column (although this could be done using the data in Table 3.2).

Test SL1 (2/16/09)					Test RL1 (2/12/09)					Test RL2 (2/18/09)				
Block, Row	Pre (lbs.)	Post (lbs.)	Δ (lbs)	Row avg. (lbs)	Block, Row	Pre (lbs.)	Post (lbs.)	Δ (lbs)	Row avg. (lbs)	Block, Row	Pre (lbs.)	Post (lbs.)	Δ (lbs)	Row avg. (lbs)
25,3	22.5	20.5	2		1,1	24.5	24	0.5		1,1	23.5	23.5	0	
26,3	22.5	21	1.5		2, 1	22	22	0		2, 1	23.5	24	-0.5	
27,3	22.5	21.5	1		3,1	22.5	23	-0.5		3,1	24	24	0	
28,3	22.5	20.5	2		4,1	23	23	0		4,1	23.5	23.5	0	
29,3	22	20	2		5,1	24	24.5	-0.5		5,1	23.5	21.5	2	
30,3	22	20.5	1.5		6,1	22.5	22.5	0		6,1	23	23.5	-0.5	
31,3	22	21	1		7,1	21.5	21.5	0		7,1	24	24	0	
32,3	22	19	3		8,1	21.5	21.5	0		8,1	23	23	0	
33,3	22	21	1		9,1	22.5	22.5	0		9,1	23.5	23	0.5	
34,3	22	20	2		10,1	23	23.5	-0.5		10,1	23	23.5	-0.5	
35,3	22	21	1		11,1	22.5	23	-0.5		11,1	23	23	0	
36,3	22	21	1	1.58	12,1	21	21	0	-0.13	12,1	23	23.5	-0.5	0.04
37,4	22	16.5	5.5		13,2	23.5	22.5	1		13,2	23	22.5	0.5	
38,4	22	17.5	4.5		14,2	22	21	1		14,2	22.5	22.5	0	
39,4	22	17	5		15,2	22	21.5	0.5		15,2	23	23	0	
40,4	22	16.5	5.5		16,2	21	19.5	1.5		16,2	22.5	22.5	0	
41,4	22	16.5	5.5		17,2	23.5	22.5	1		17,2	23	21	2	
42,4	22	17	5		18,2	21.5	21	0.5		18,2	22.5	22.5	0	
43,4	22	16.5	5.5		19,2	22.5	22	0.5		19,2	22.5	22.5	0	
44,4	22	13	9		20,2	20.5	20	0.5		20,2	22.5	22	0.5	
45,4	21.5	16.5	5		21,2	21	20.5	0.5		21,2	22.5	22	0.5	
46,4	21.5	16.5	5		22,2	20.5	20	0.5		22,2	22.5	22.5	0	
47,4	21.5	13	8.5		23,2	22	22	0		23,2	22.5	23	-0.5	
48,4	21.5	13.5	8	6.00	24,2	20	20	0	0.63	24,2	22.5	22	0.5	0.29
49,5	21.5	14	7.5		25,3	22	13.5	8.5		25,3	22	16	6	
50,5	21.5	15	6.5		26,3	21	13.5	7.5		26,3	22	15	7	
51,5	21.5	9.5	12		27,3	21	15	6		27,3	21.5	16.5	5	
52,5	21.5	14.5	7		28,3	21	13	8		28,3	22	16.5	5.5	
53,5	21.5	16	5.5		29,3	20	15	5		29,3	22	14	8	
54,5	21.5	14.5	7		30,3	21.5	16	5.5		30,3	22.5	15	7.5	
55,5	21	14	7		31,3	22	17	5		31,3	22.5	16	6.5	
56,5	21	14.5	6.5		32,3	19.5	13.5	6		32,3	22.5	15.5	7	
57,5	21	10.5	10.5		33,3	22	16	6		33,3	22.5	17	5.5	
58,5	21	14	7		34,3	21	16	5		34,3	22	15.5	6.5	
59,5	21	9	12		35,3	21	13.5	7.5		35,3	22	16.5	5.5	
60,5	21	10	11	8.29	36,3	21	12.5	8.5	6.54	36,3	22.5	16.5	6	6.33
61,6	21	10	11		37,4	12.2*	19	1.5		37,4	14.2*	19	2.5	
62,6	21	14.5	6.5		38,4	14.3*	20	1.5		38,4	13.5*	17	4	
63,6	21	14.5	6.5		39,4	14.6*	18.5	2		39,4	11.9*	17	3	
64,6	21	14	7		40,4	12.4*	19	1		40,4	13.8*	18.5	3	
65,6	21	15	6		41,4	13.4*	19.5	1		41,4	13.2*	18	2.5	
66,6	21	14.5	6.5		42,4	14.2*	19.5	1		42,4	12.7*	16.5	4	
67,6	21	8	13		43,4	14.7*	20.5	1.5		43,4	12.7*	18.5	2	
68,6	21	14	7		44,4	13.7*	19	1.5		44,4	14.3*	18	3.5	

Block, Row	Pre (lbs.)	Post (lbs.)	Δ (lbs)	Row avg. (lbs)	Block, Row	Pre (lbs.)	Post (lbs.)	Δ (lbs)	Row avg. (lbs)	Block, Row	Pre (lbs.)	Post (lbs.)	Δ (lbs)	Row avg. (lbs)
69,6	21	15	6		45,4	13.3*	20	1.5		45,4	13.0*	18.5	2.5	
70,6	20.5	13	7.5		46,4	13.0*	18.5	1		46,4	13.0*	17.5	3.5	
71,6	20.5	8	12.5		47,4	12.9*	19	1		47,4	13.0*	16.5	4.5	
72,6	20.5	14	6.5	8.00	48,4	13.2*	17.5	1	1.29	48,4	15.4*	18	3.5	3.21
73,7	12.7*	12.5	8		**total**	945.4	845.4	-100		**total**	978.7	860.2	-119	
74,7	17.1*	13.5	7		**avg**	19.7	17.61	-2.08		**avg**	20.39	17.92	-2.47	
75,7	14.6*	11	9.5											
76,7	14.6*	14.5	6											
77,7	14.3*	16.5	3.5											
78,7	14.8*	10.5	9.5											
79,7	14.3*	11	9											
80,7	15.7*	14.5	5.5											
81,7	15.2*	14.5	5.5											
82,7	14.5*	15	5											
83,7	12.5*	12	7.5											
84,7	13.0*	12.5	7	6.92										
total	1207	837.4	-370											
avg	20.12	13.96	-6.16											

* Top row of blocks – weights corrected by subtracting weight of unwetted portion

Table 3.2. Pre- and post-test block weights. Note that the bottom two rows of blocks from Test SL1 were undissolved and therefore not removed and weighed (except for a few spot checks not listed in this table), and were reused for the Test RL2. The red entries indicate mass gain which is thought to be due to accuracy of the Taylor TE-400 digital scale used (±0.5 lb).

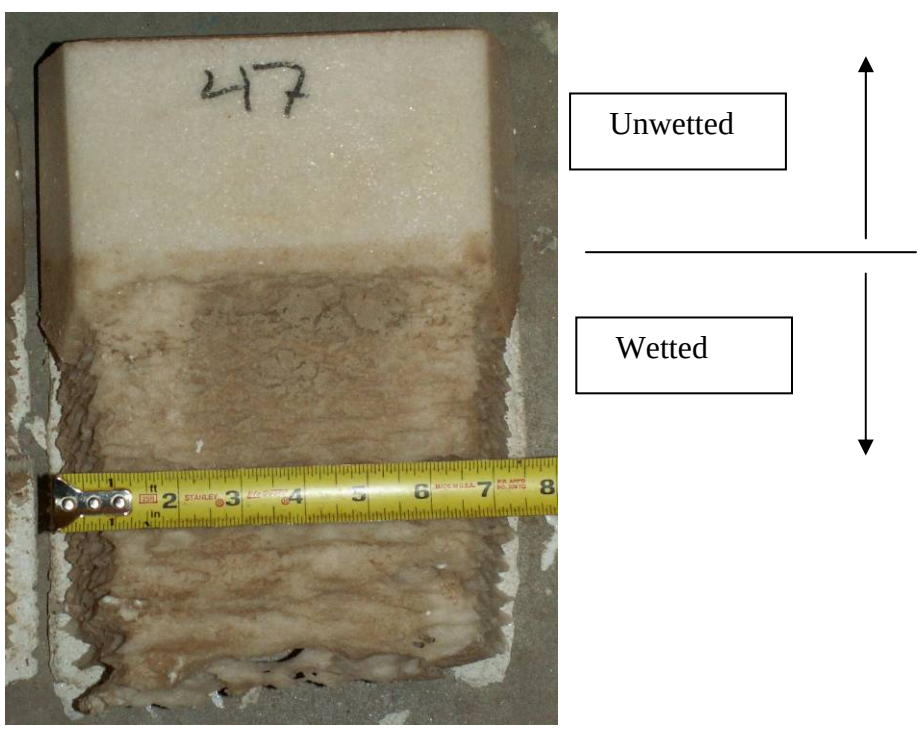

Figure 3.9. Salt block from top row of blocks during Test RL2. This shows the unwetted portion of the block whose weight is estimated and compensated for in the data shown in Table 3.2.

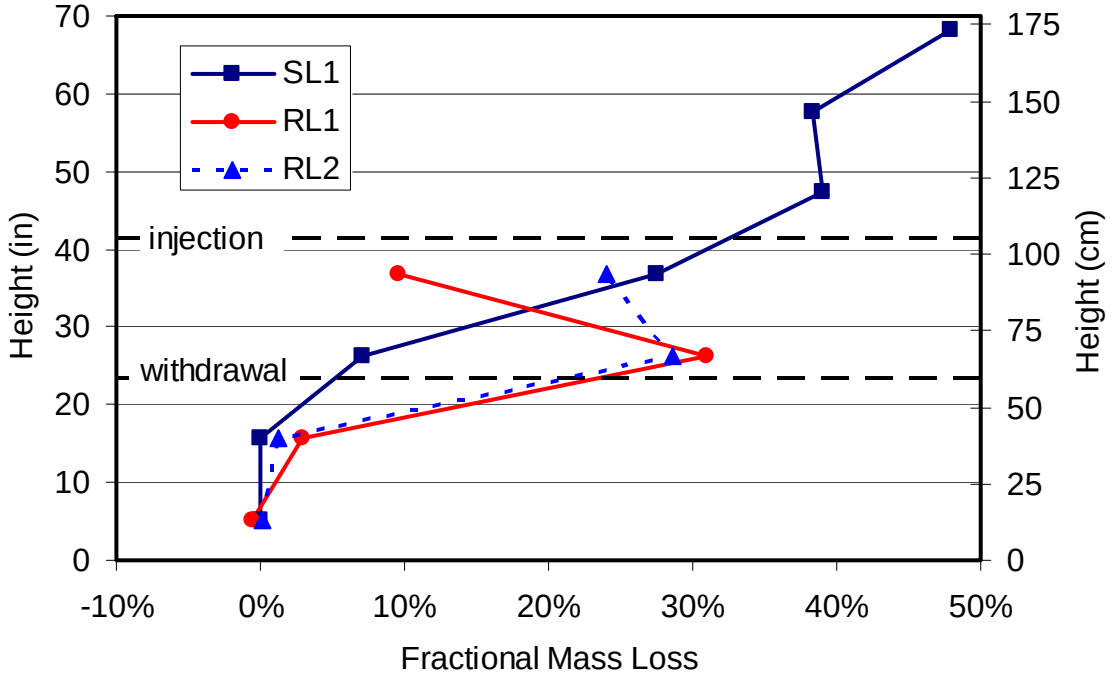

Figure 3.10. Row-averaged mass loss as a function of height in the tank (plotted at center of each row of salt blocks). Data are from Table 3.2. Note that injection and withdrawal depths are only valid for test SL1.

71
60
59
57
48
47
46
45
02.17.2009
36
35
34
33

67
44
43
42
41
02.17.2009
32
31
30
29

Figure 3.11. Shape of the upper five rows of salt blocks removed from tank following Test SL1. The bottom two rows of salt blocks were undissolved (several weights checked to verify this) and were reused in the next test (RL2). See Table 3.2 for the pre- and post-test block weights.

Figure 3.12. Shape of the four rows of salt blocks removed from tank following first remedial leach test (RL1). See Table 3.2 for the pre- and post-test block weights.

Figure 3.13. Shape of the four rows of salt blocks removed from tank following second remedial leach test (RL2). See Table 3.2 for the pre- and post-test block weights. There is much more dissolution in the upper rows for this test than in the Test RL1.

Conductivity/temperature profiles

As indicated in Figures 2.1 and 2.2, three temperature/conductivity probes were traversed vertically in the tank during these tests to measure profiles of the local temperature and conductivity. The probes are Microscale Conductivity and Temperature Instruments (MSCTI) from Precision Measurement Engineering, Inc., Carlsbad, CA, shown in Figure 3.14. The probe locations relative the tank centerline injection and withdrawal tubes are shown in Figure 3.15. The probes were traversed throughout the tests, but were stopped for 20 seconds prior to each data acquisition. The traverse motion and the data acquisition were controlled through a LabVIEW program. The instantaneous depths of the probes during the remedial leach tests were shown previously in Figure 2.4, and the depths for Test SL1 are shown in Figure 3.16.

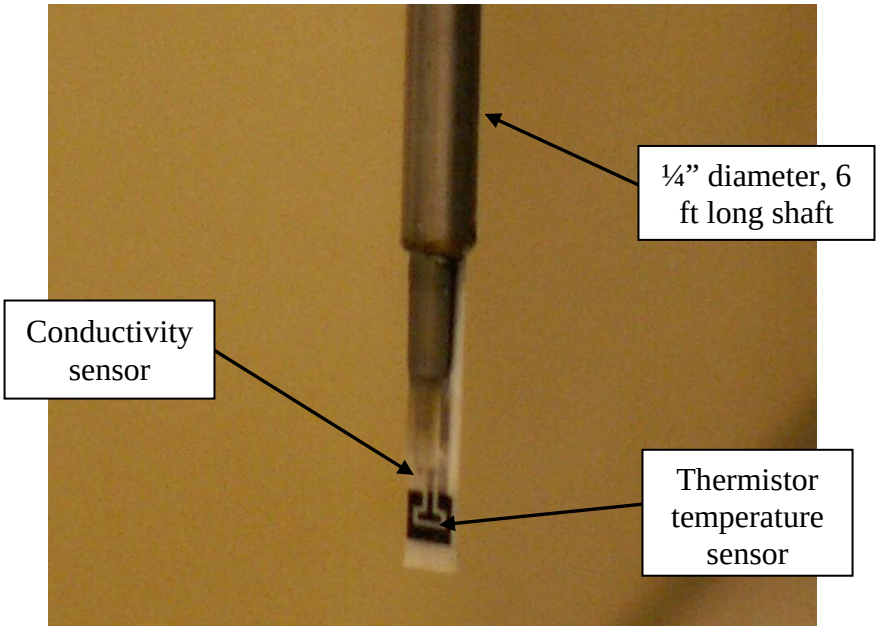

Figure 3.14. Microscale Conductivity/Temperature Probe from Precision Measurement Engineering.

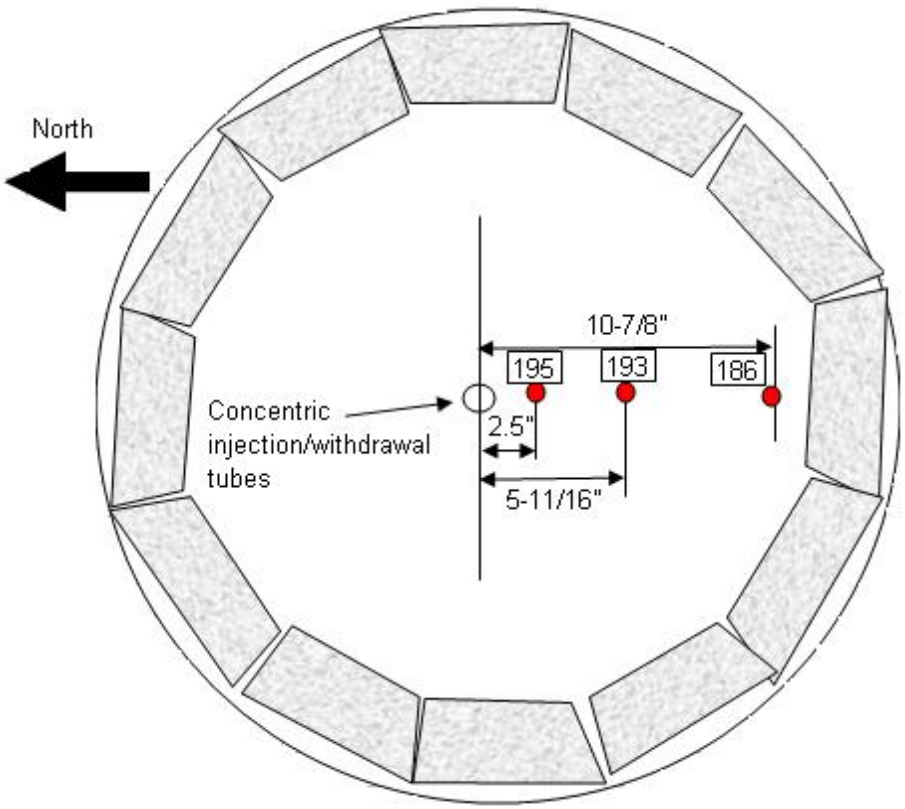

Figure 3.15. Probe locations in tank. Probe numbers (186, 193, 195) correspond to preamplifier/excitation electronics.

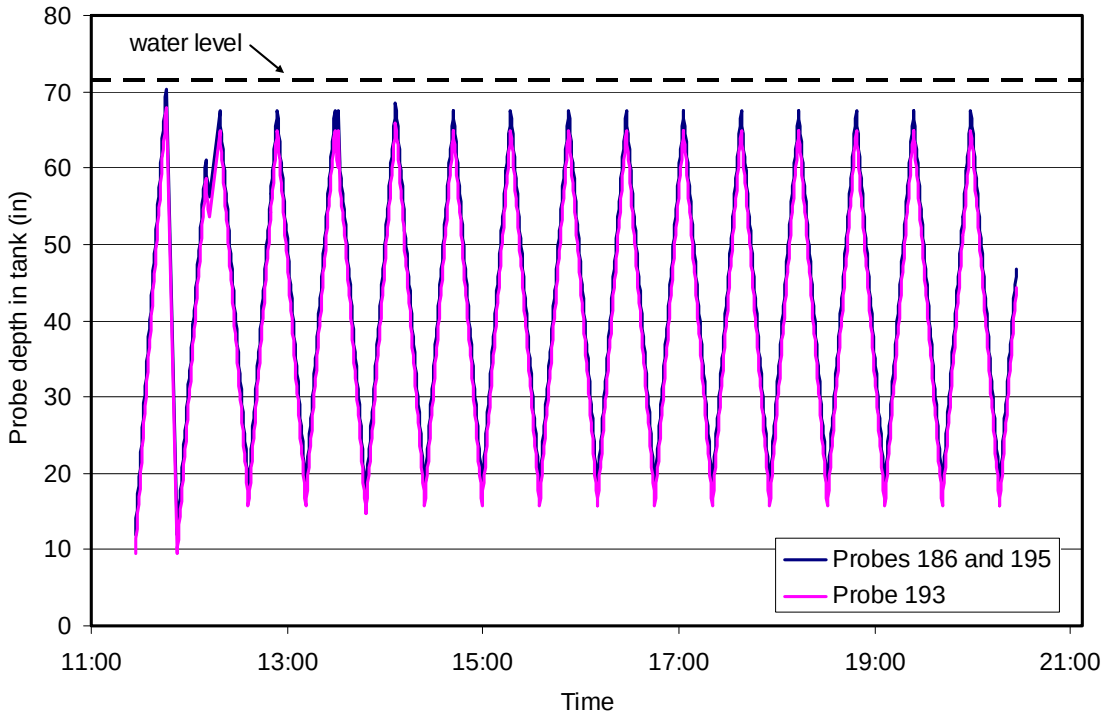

Figure 3.16. Probe locations in tank during Test SL1.

The raw data from these tests were converted from voltages to conductivity and temperature using calibration data recorded prior to the tests. The temperature calibration is quite stable and only needs to be checked occasionally. This was done the week before testing. The temperature calibration data is shown in Figure 3.17. The conductivity calibration is more sensitive, and must be done on the day of each test. Figures 3.18 through 3.20 show the conductivity (expressed as % NaCl saturation) calibration for each of the tests. These were performed using premixed solutions of water and pure NaCl at room temperature. Note that calibration was not performed using solutions with the actual composition of the salt blocks, which contained impurities in addition to NaCl.

The conversion from voltage to conductivity required use of a calibration curve that was determined from a curve fit to the pure NaCl calibration data. It has been seen that the curve does not capture every conversion perfectly, and even applying the calibration curve to the calibration data can yield errors on the order of ±5%.

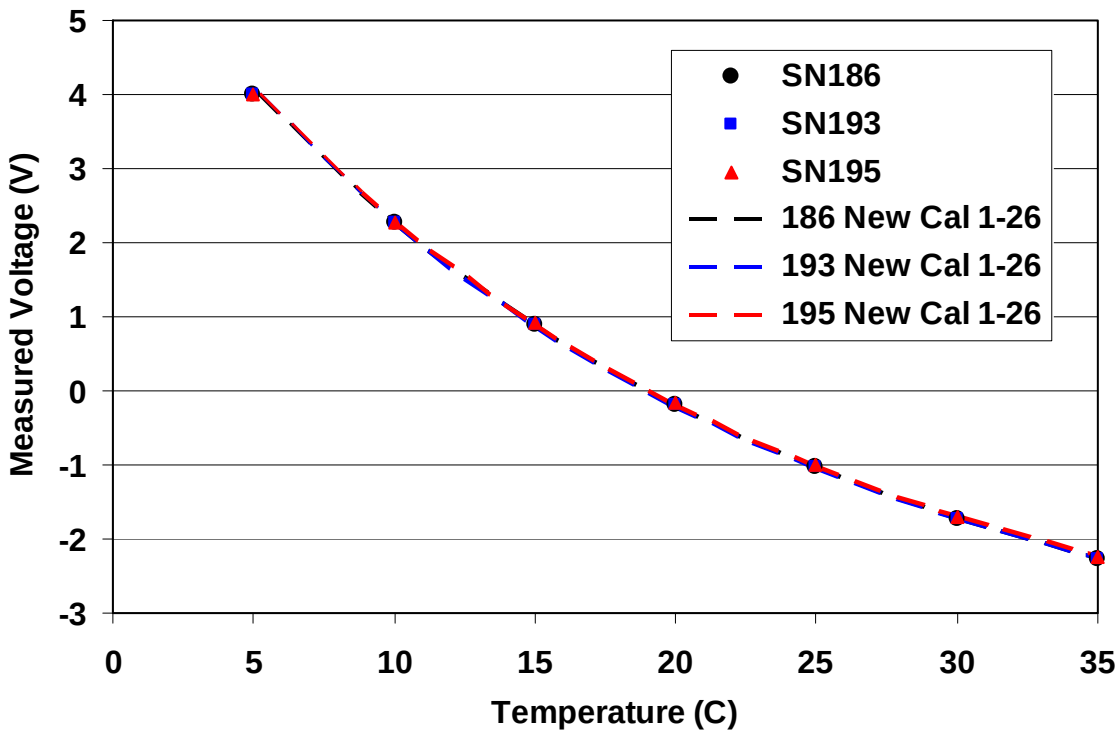

Figure 3.17. Temperature calibration data for all three MSCTI probes, performed 1/26/09 prior to testing. Temperature calibration is quite stable and only needs an occasional check. The points in this figure are the measured values and the dashed lines are the curve fits used in the temperature data conversion.

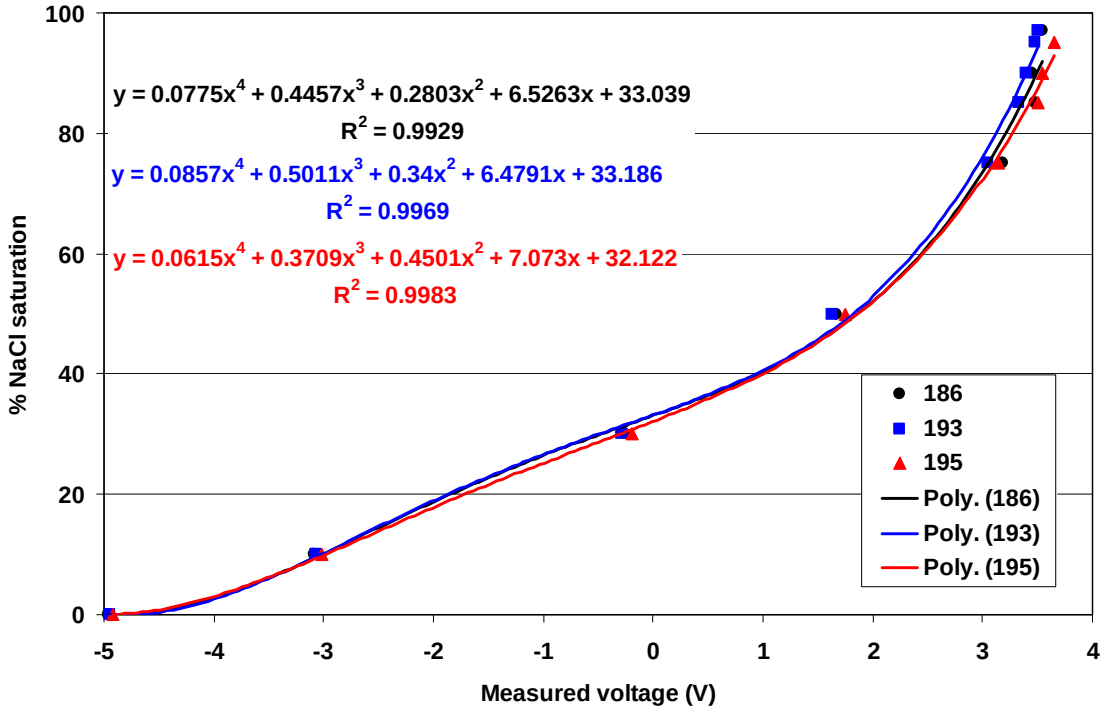

Figure 3.18. Conductivity calibration data for all three MSCTI probes performed immediately prior to Test SL1, before installing probes in tank. The polynomial fits are the calibration curves used to convert measured voltages to NaCl saturation level.

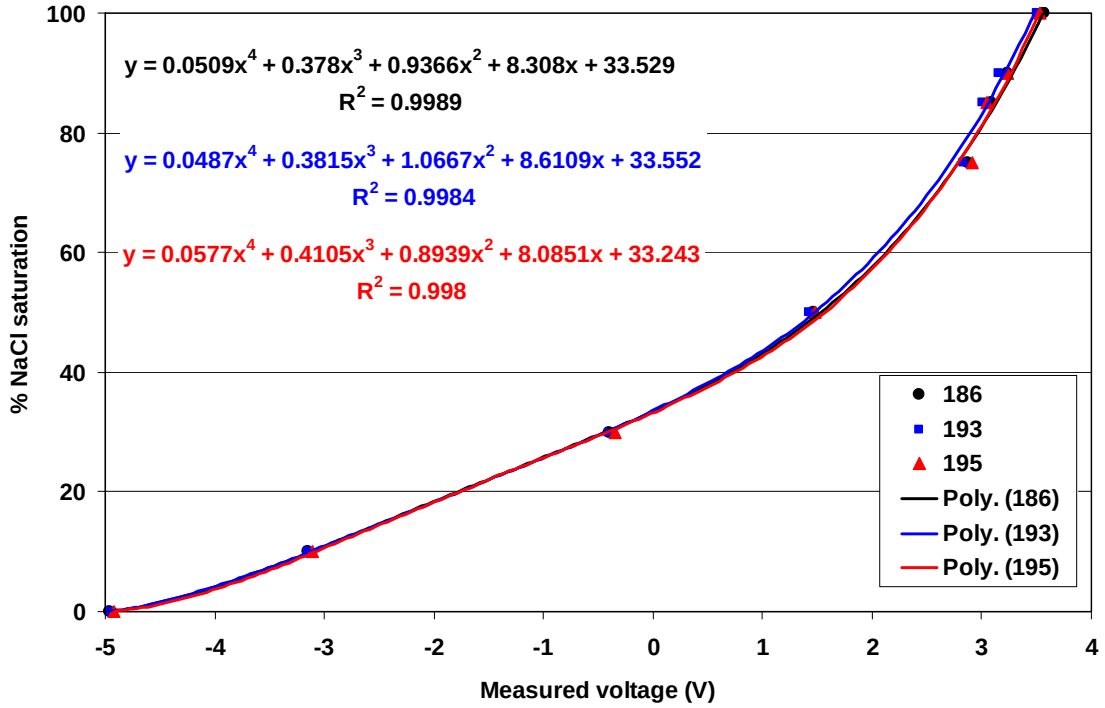

Figure 3.19. Conductivity calibration data for all three MSCTI probes performed immediately prior to Test RL1, before installing probes in tank. The polynomial fits are the calibration curves used to convert measured voltages to NaCl saturation level.

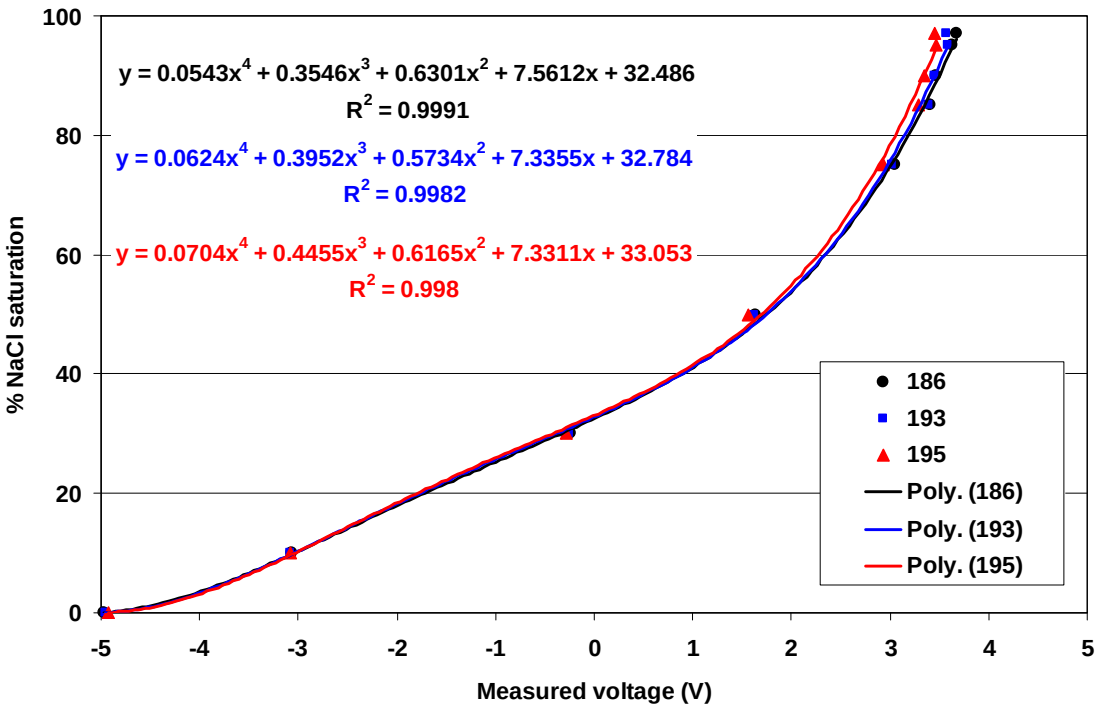

Figure 3.20. Conductivity calibration data for all three MSCTI probes performed immediately prior to Test RL2, before installing probes in tank. The polynomial fits are the calibration curves used to convert measured voltages to NaCl saturation level.

Representative temperature profiles for the 3 tests are shown in Figures 3.21 through 3.23. These show that the temperature was fairly stable, declining slightly over the run times. Figure 3.21 shows that in test SL1 the upper fluid was well-mixed, with fairly uniform temperature about the injection depth, with a pronounced temperature gradient between the injection and withdrawal locations. The overall temperature range over the 9 hour test was approximately 4°C. Figure 3.22 shows the temperature data for test RL1, showing good uniformity both above and below the injection/withdrawal depth, but a gradient near that depth. The overall temperature range over the 5 hour test was approximately 4°C. Figure 3.23 shows the temperature data for test RL2, indicating uniform, constant temperature below the withdrawal depth and a continuous temperature decline above that depth, with fairly similar behavior during injection and withdrawal. The overall temperature range over the 6 hour test was approximately 2°C.

The conductivity profiles are shown in Figure 3.24 through 3.32 for each of the three probes and three tests. The "raw" converted conductivity values gave unphysical results. Despite the fact that the calibrations seemed to work well and provided a smooth conversion curve (see Figures 3.18 to 3.20), in every test the measured NaCl saturation level at the start of the test was greater than 100%, ranging from 1.3 to 1.6 times fully saturated. Based on these unexpected findings, a closer examination of the conductivity/temperature data was undertaken. The early analysis of the data had assumed that changes in temperature of the simulated cavern system during the experiments was negligible, based on the data in Figures 3.21 to 3.23. However, it was apparent that changes in the temperature of the system would have to be taken into account to determine accurately the conductivity of the brine-water mix, especially changes in temperature between the calibration baths and the actual tests. To this end, the actual temperature of the brine-water

mix at the sensor location was computed via a Matlab program which was developed to compare the data taken during a calibration just prior to each experiment with the experimental data to find an equation relating the raw output voltages to localized temperature. The final data analysis was performed using the corrected temperature and salinity values output by this program. This was needed because conductivity is a strong function of temperature, so even small changes in temperature can lead to significant changes in conductivity.

Figures 3.24 through 3.26 show the corrected conductivity data from Test SL1, converted to NaCl saturation (0 to 100% of saturation) using the pretest calibration data shown in Figure 3.18. The concentration starts fairly uniform at approximately fully saturated conditions, and showed a steady decline with time. Above about 35 inches (higher in tank), the data are tightly grouped and fairly constant at each time, indicating good mixing. Below that level the downward trends are identical but the average concentration values are increasingly closer to saturation the deeper in the tank (closer to the floor) that data are taken, with a stronger gradient than higher in the tank. There are no significant radial variations in the conductivity data (i.e., the data from the three probes are fairly similar).

Figures 3.27 through 3.29 show that there are two major groupings of the data from Test RL1, those at depths low in the tank and those at depths high in the tank. The dividing line seems to be at about 20 inches, or 3 inches below the injection/withdrawal depth. The values in the lower depth grouping started high (near saturation) then steadily decreased with time as fresh water was added to the tank, while those in the higher depth group started at low saturation levels and increased until they approached the saturation values of the lower depth measurements. At the time that the flow was reversed from injection to withdrawal, all of the higher depth values spiked higher (towards saturation), and continued to increase as water was pumped out of the tank. There do not seem to be significant variations with position across the tank (the three different probes).

Figures 3.30 through 3.32 show that there are also two major groupings of the data from Test RL2, those at depths low in the tank and those at depths higher in the tank. The dividing line again seems to be at about 20 inches. The values in the lower depth grouping started consistently high (near saturation) then steadily decreased with time as fresh water was added to the tank, with no clear demarcation of the times that injection ended, the tank sat undisturbed for an hour, or withdrawal started. Those in the higher depth group started at low saturation levels and increased until they approached the saturation values of the upper measurements. The rate of increase was generally highest during injection, slowed during the one hour rest period, then decreased again during withdrawal.

For all of the tests the middle probe (193, approximately halfway between the center injection/withdrawal location and the salt walls) seemed to indicate a tighter grouping of concentration below the injection point than that seen by the other two probes. This is thought to be unique to this probe, not caused by local flow characteristics. This will be evaluated further prior to next use of the probes.

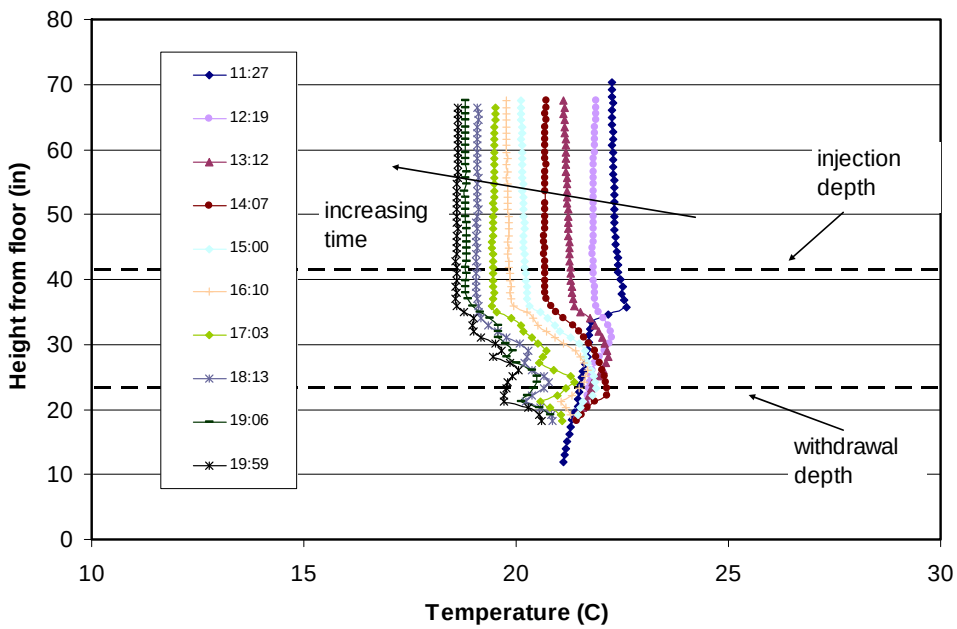

Figure 3.21. Temperature profiles: Probe 195, Test SL1 (probes 186 and 193 very similar for this test). The legend shows depth in tank at which data were taken, measured up from the tank floor. The upper dashed line indicates the depth of the injection line and the lower dashed line the depth of the withdrawal line.

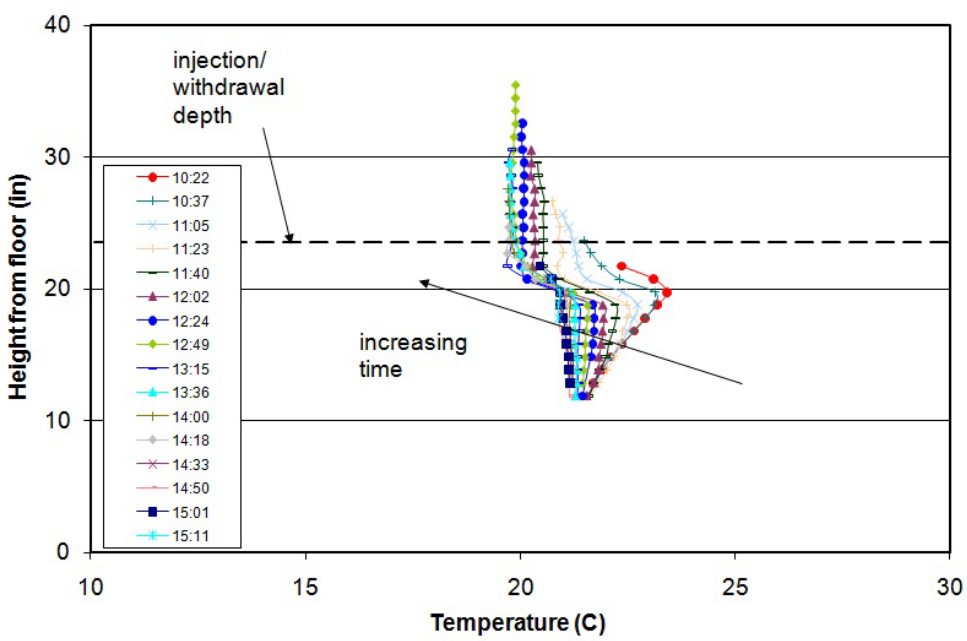

Figure 3.22. Temperature profiles: Probe 186, Test RL1 (probes 193 and 195 very similar for this test). The legend shows times at which data were taken. Flow was reversed from injection to withdrawal at 12:45 (2.5 hours after start of injection).

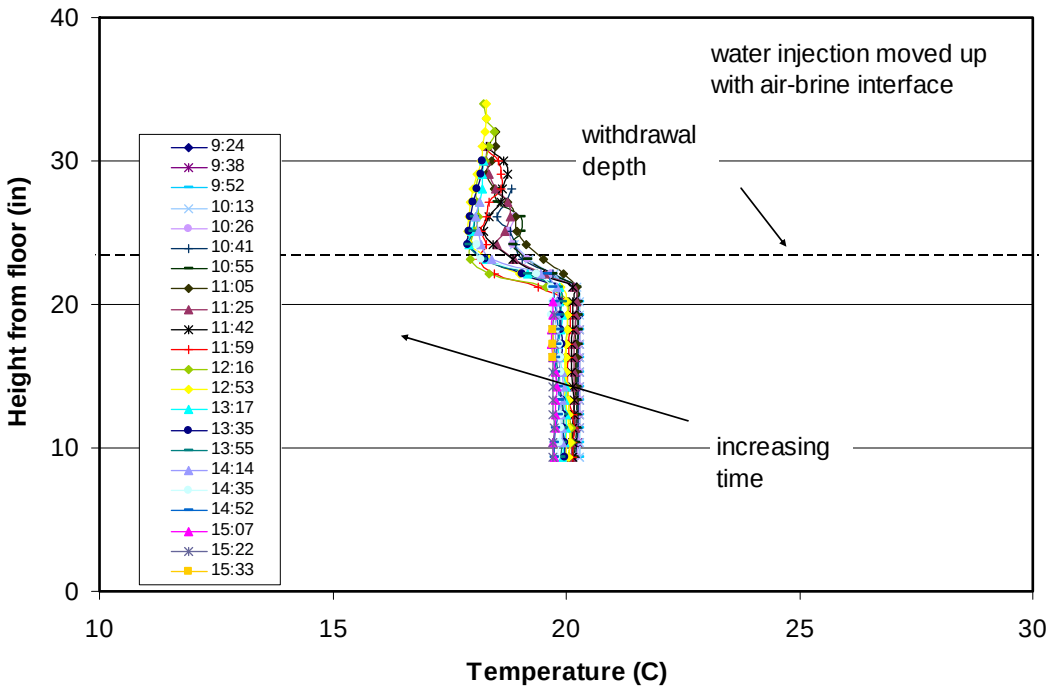

Figure 3.23. Temperature profiles: Probe 193, Test RL2 (probes 186 and 195 very similar for this test). The legend shows depth in tank at which data were taken, measured up from the tank floor. Injection stopped at 11:53, withdrawal started at 12:55.

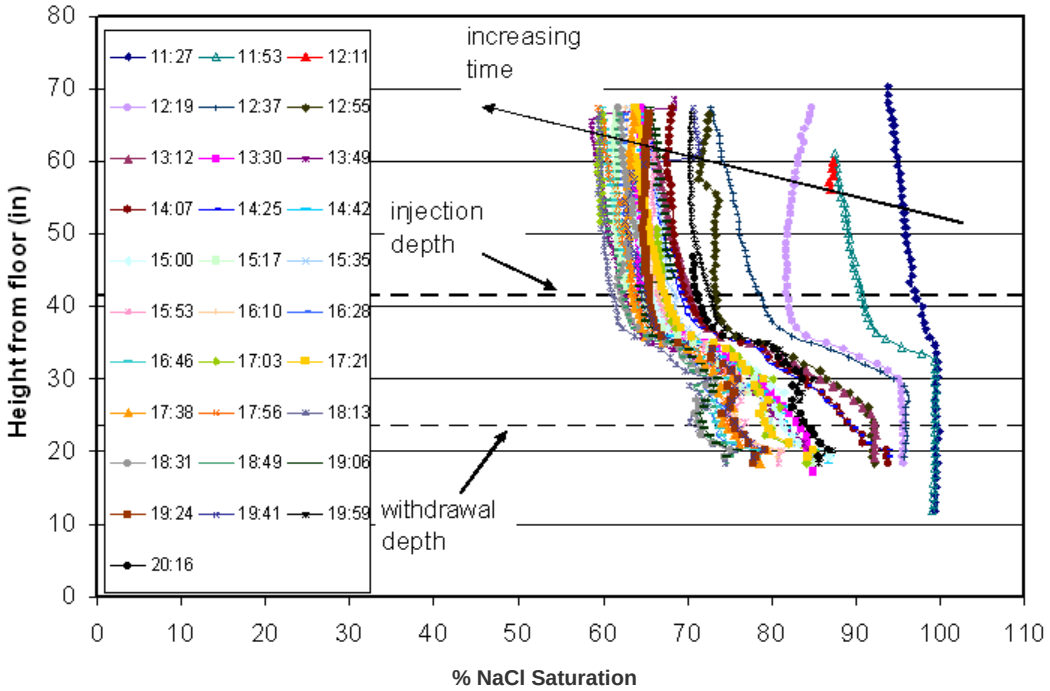

Figure 3.24. Concentration profiles: Probe 186, Test SL1. Legend shows time data were taken. Conductivity data have been corrected for temperature changes during test and between calibration and test.

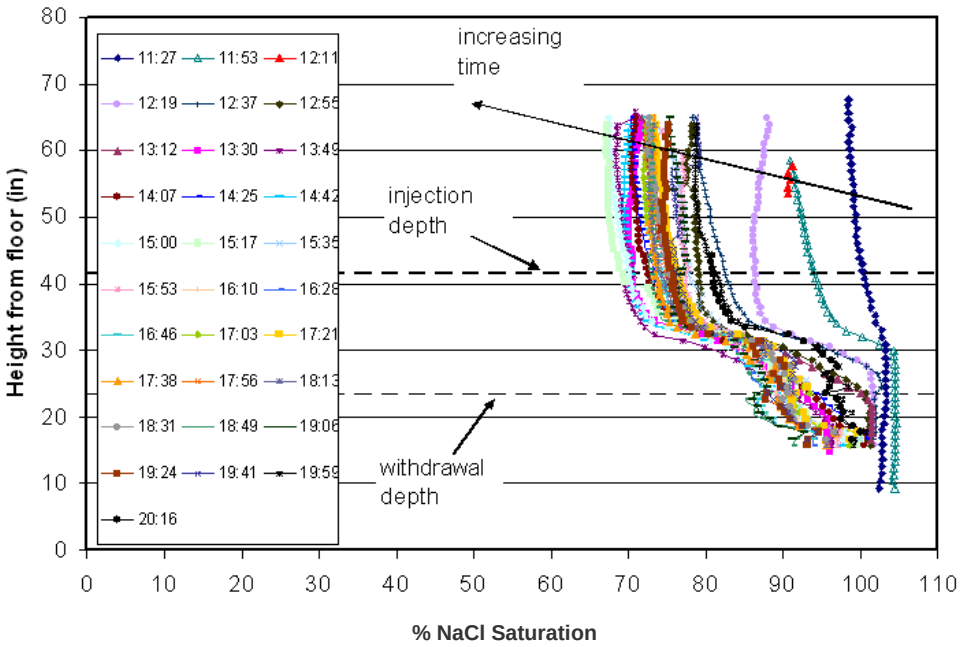

Figure 3.25. Concentration profiles: Probe 193, Test SL1. Legend shows time data were taken. Conductivity data have been corrected for temperature changes during test and between calibration and test.

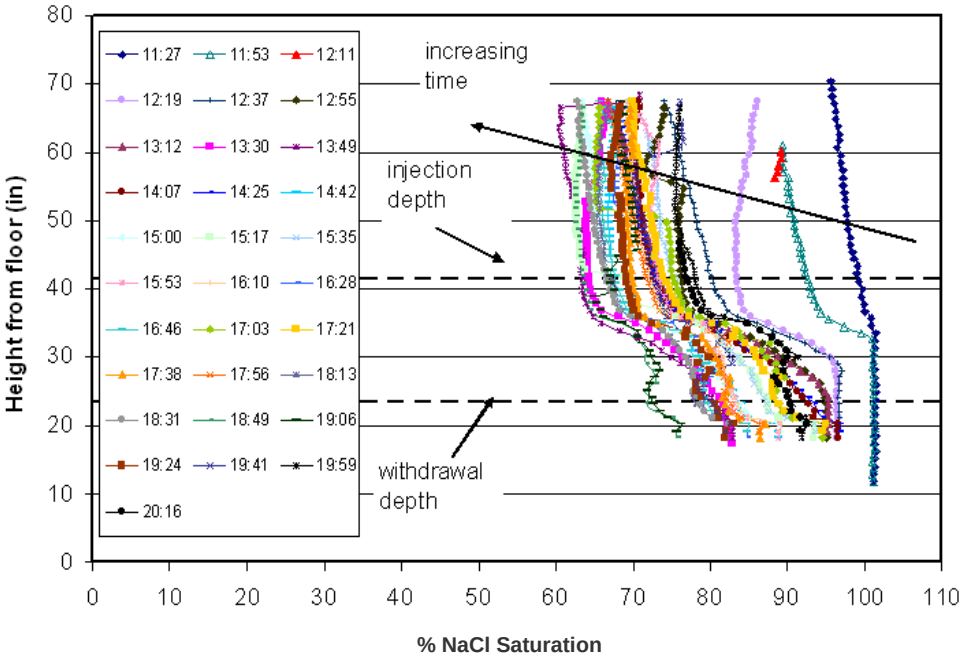

Figure 3.26. Concentration profiles: Probe 195, Test SL1. Legend shows time data were taken. Conductivity data have been corrected for temperature changes during test and between calibration and test.

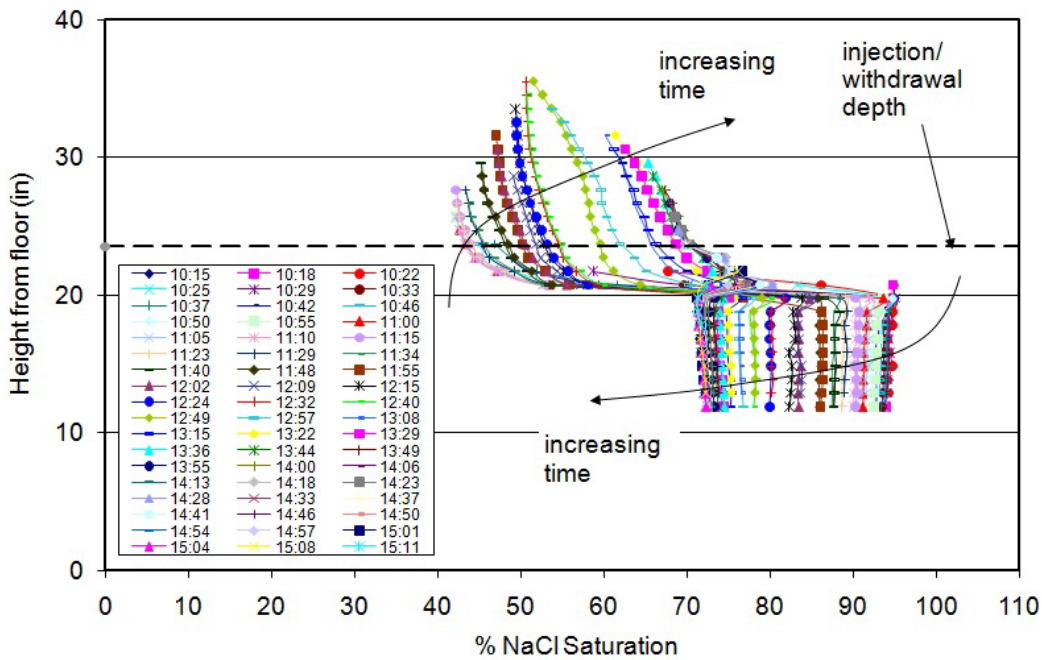

Figure 3.27. Concentration profiles: Probe 186, Test RL1. Legend shows time data were taken. Flow was reversed from injection to withdrawal at 12:45 (2.5 hours after start of injection). The dashed line indicates the depth of the injection/withdrawal line. Conductivity data have been corrected for temperature changes during test and between calibration and test.

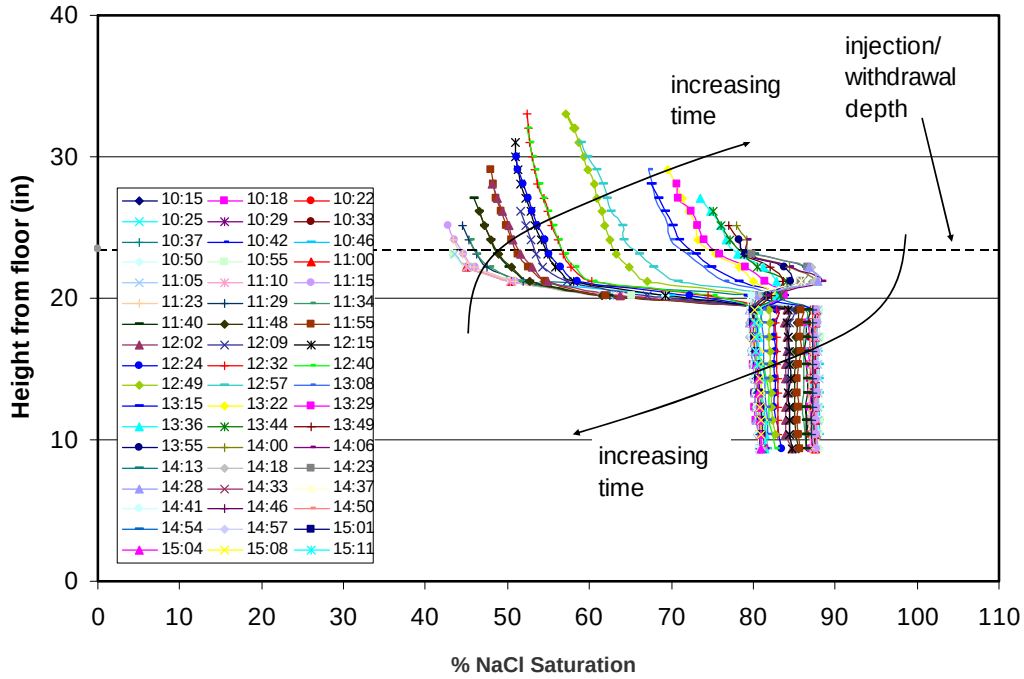

Figure 3.28. Concentration profiles: Probe 193, Test RL1. Legend shows time data were taken. Flow was reversed from injection to withdrawal at 12:45 (2.5 hours after start of injection). Conductivity data have been corrected for temperature changes during test and between calibration and test.

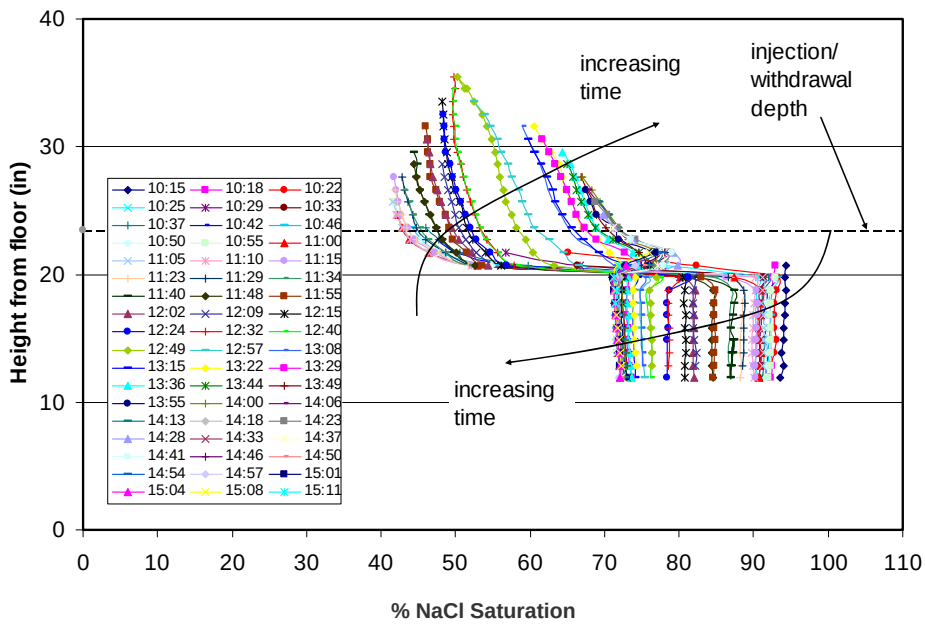

Figure 3.29. Concentration profiles: Probe 195, Test RL1. Legend shows time data were taken. Flow was reversed from injection to withdrawal at 12:45 (2.5 hours after start of injection). Conductivity data have been corrected for temperature changes during test and between calibration and test.

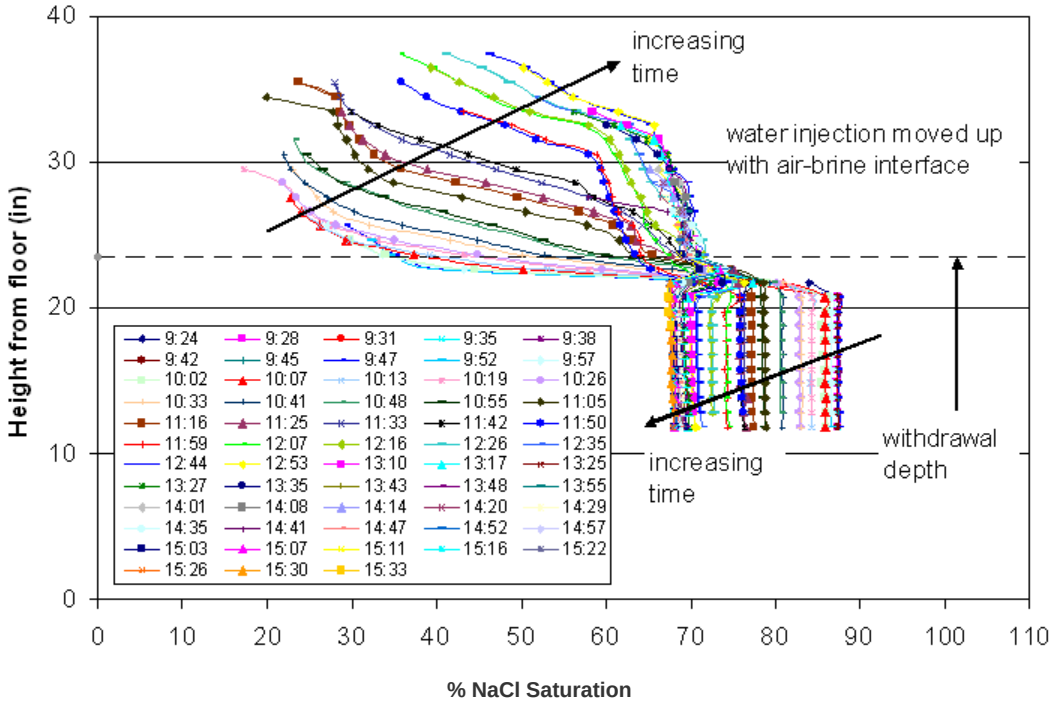

Figure 3.30. Concentration profiles: Probe 186, Test RL2. Legend shows time data were taken. Injection stopped at 11:53, withdrawal started at 12:55. The dashed line indicates the depth of the withdrawal line. Conductivity data have been corrected for temperature changes during test and between calibration and test.

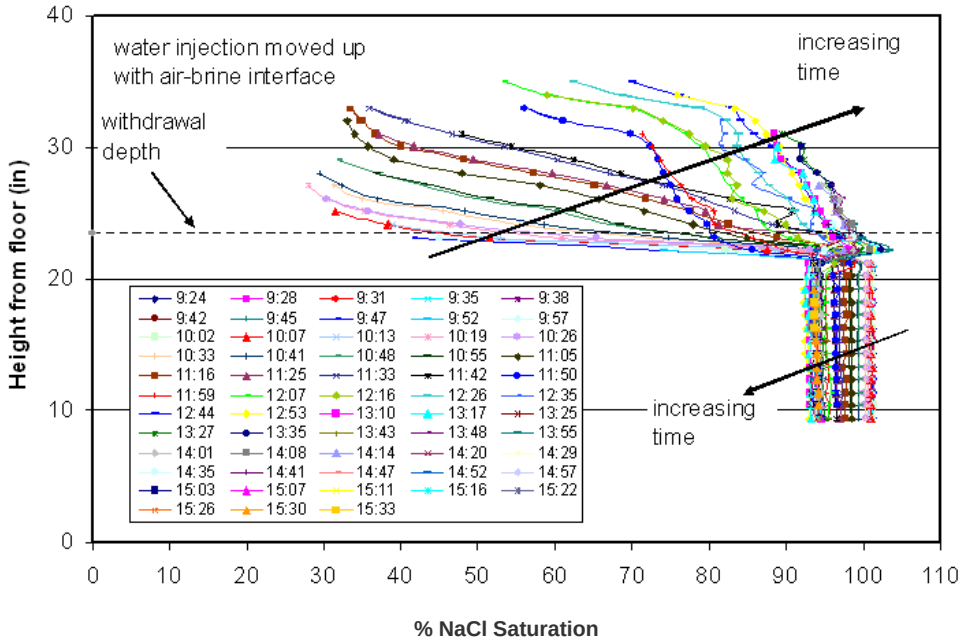

Figure 3.31. Concentration profiles: Probe 193, Test RL2. Legend shows time data were taken. Injection stopped at 11:53, withdrawal started at 12:55. Conductivity data have been corrected for temperature changes during test and between calibration and test.

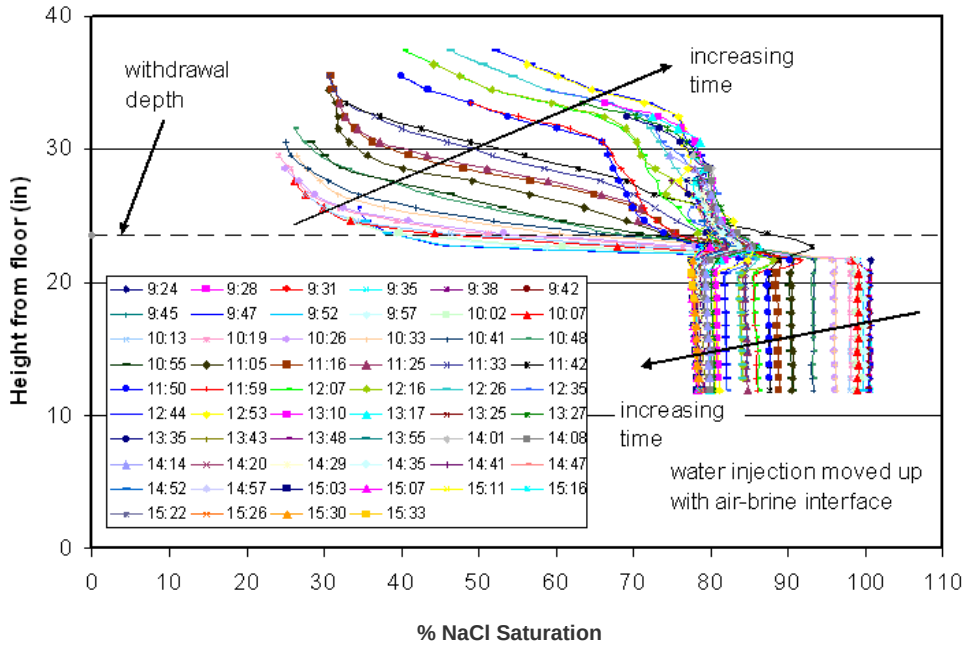

Figure 3.32. Concentration profiles: Probe 195, Test RL2. Legend shows time data were taken. Injection stopped at 11:53, withdrawal started at 12:55. Conductivity data have been corrected for temperature changes during test and between calibration and test.

Salt Mass Balances

Table 3.3 summarizes the salt mass balances for each test. The initial and final mass of the salt blocks comprising the walls was measured by weighing (see Table 3.2). The amount of salt removed from the system during each test was calculated by integrating the outflow density, flowrate, and time values. The mass of salt in the brine at the start of the test was estimated based on the average initial diameter of the brine-filled cavity and known amount of salt in the saturated brine (density 1.2 g/cc, salt 0.32 g/cc, water 0.88 g/cc). The estimated final mass of salt in the unsaturated brine post-test was calculated using an average 75% saturation level (from probe data, Figures 3.24-3.32), and larger liquid volume based on average wall dissolution. The results are shown in Table 3.3, which indicate a reasonable mass balance. The change in mass of loose salt on the tank floor could not be estimated because the brine was opaque, but Figure 3.33 indicates that it did not all dissolve during test SL1, and similar remnant salt was observed in tests RL1 and RL2.

	Initial Salt Mass (kg)			Final Salt Mass (kg)				Difference (kg)
Test	**Walls**	**Brine**	**Total**	**Walls**	**Brine**	**Pumped Out**	**Total**	**Initial-Final**
SL1	**548.6**	**174.4**	**723.0**	**380.6**	**133.5**	**180.5**	**694.6**	**28.4**
RL1	**429.7**	**57.2**	**486.9**	**384.3**	**43.5**	**47.9**	**475.7**	**11.2**
RL2	**444.9**	**57.2**	**502.1**	**391**	**44.3**	**52.3**	**487.6**	**14.5**

Table 3.3. Initial and final salt mass in the system for each test. Uncertainties in the estimated liquid values are due to uncertainties in the exact brine volume (based on wall thicknesses before and after dissolution) and in the final brine concentration in the tank post-test.

Figure 3.33. Photo showing salt walls and tank floor after test SL1.

There are a number of issues with the mass balance. First, the final tank saturation of 75% seems reasonable, but that value may be suspect given some of the differences in the profiles between the three radial probe locations. Higher values of the final tank saturation reduce the final difference significantly. For example, if the final tank saturation is assumed to be 85%, the difference for the three experiments is reduced to 7.9, 4.5, and 7.7 kg for tests SL1, RL1, and RL2, respectively. The difference in the probe readings needs to be addressed in any future experiments. The second issue is the salt on the tank floor, which was about 23 kg (50 lb) at the start of each test. The change in the salt mass on the floor was not measured, but it definitely wasn't all dissolved as seen in Figure 3.33. In the future, separate salt blocks might be placed on the floor that will be weighed before and after each test. In any event, the salt mass balance shows reasonable agreement given the uncertainties of the information.

4. Discussion

New diagnostics applied in this test included the traversed conductivity probes and the ultrasonic transducers. Both worked but had issues that should be resolved before the next series of tests. Also, an underwater camera was added but it did not work well enough to justify its continued use since moving the camera affected the ultrasonic measurements.

For the conductivity probes, the calibration issues that led to converted values above fully saturated must be resolved. This was handled in these tests by normalizing to the maximum values. Calibration with salt blocks present will be tested to see whether some component of the undissolved salt blocks shifts the calibration curves.

The ultrasonic transducers worked very well in Test SL1 but had unexpected results, including apparent thickening of the salt blocks, in Tests RL1 and RL2. The RL1 problems were thought to be due to the ultrasonic transducers moving when other operations jostled them during the test, but those were eliminated for the later tests. It is possible that the salt blocks shifted or settled slightly during the tests, which could cause jumps in the data, but there is no easy explanation for the apparent thickening. A possible improvement would be to support the transducers from the salt blocks themselves so any salt block motion would move the transducer by the same amount.

Two types of tests were performed, standard (SL1) and remedial (RL1 and RL2) leaching. The data showed much more salt wall dissolution and better mixing between the injected water and the resident brine in the SL1 test. The RL1 tests showed two separate well mixed zones while RL2 shows more continuous mixing. These differences are probably due to the water injection problems in test RL2. During the withdrawal period, the fluid becomes more mixed.

For all tests, the conductivity probes showed two major groupings of the data; those acquired deep in the tank and those acquired higher in the tank. For the RL tests the deeper group was more consistent while for the SL test the upper group seemed more uniform.

5. Conclusions

Sandia National Laboratories conducted a series of salt wall leaching experiments in early 2009. Three tests were run, one a "standard" leaching test in which fresh water was pumped into a brine-filled cavity with salt walls while mixed fluid was withdrawn at the same rate, and two "remedial" leaching configurations in which fresh water was added to an existing brine layer in the salt-walled tank with no withdrawal until a predetermined fill level was achieved at which time the mixed fluid was either withdrawn at the same rate as injection (Test RL1) or allowed to sit for one hour prior to withdrawal (Test RL2). In all tests, diagnostics included measurement of the injection and withdrawal flow rates, lab temperature, water conductivity and temperature profiles at three locations, and salt dissolution measurements by ultrasound, before and after weights, and an underwater camera (Test RL1 only). The use of these diagnostics gave leaching data sets that include much more detailed salt wall dissolution data than obtained in previous tank experiments (O'Hern et al., 2008). These data will be used to evaluate mechanistic CFD leaching models.

The results show that:

1. **Weighing the salt blocks seemed to yield useful data.** This is fairly easy and gave results consistent with photographs. The measured wall salt mass loss, combined with estimated liquid salt mass lost, gave reasonable agreement with estimated salt removed by water exchange (within uncertainty due to estimated average initial and final wall thickness and choice of final brine saturation).

2. **Conductivity/temperature data consistent:** Accurate conductivity data require that the raw data be corrected for temperature variations during the test and between calibration and test temperatures. For the test conditions used in these 3 tests, there seemed to be only minor differences in temperature or conductivity with radial location. However, probe calibration should be performed using solutions containing the same composition as the dissolved salt blocks for more accurate tank measurements. In addition, a post-test calibration check should be performed to check the validity of the probe calibration over the time required for each test.

3. **Standard leach configuration:** As expected, the initially saturated brine steadily mixed with the injected fresh water over the course of this test. The mass loss of the salt walls increased fairly uniformly with increasing height in the tank. For the run time used here there was no measurable mass loss for the bottom 2 rows (about 21 inches) of the salt walls.

4. **Remedial leach configuration.** Most mass loss was in the third row of blocks since they were exposed to fresh water for the longest time. The conductivity data showed two distinct well mixed regions in the tank, roughly above and below the injection location. The inadvertent injection at the rising free surface in Test RL2 caused less fluid mixing and higher salt wall dissolution.

5. **Not all salt blocks are the same.** Observations and post-test photographs demonstrate significant block-to-block variability, with neighboring blocks on the same row dissolving at significantly different rates.

The facility and diagnostics are in place for possible future testing. In addition, the facility can be reconfigured for examination of different flow geometries, as needed.

Appendix A – Ultrasonic Data for Test SL1

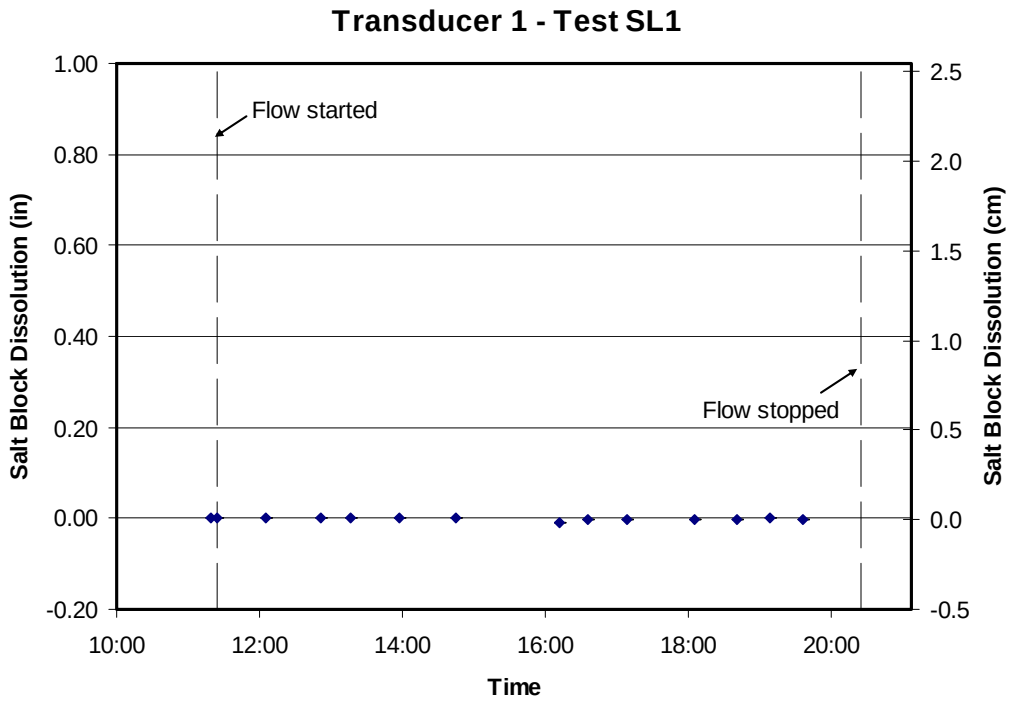

Figure A.1. Ultrasonic data for ultrasonic transducer 1, Test SL1.

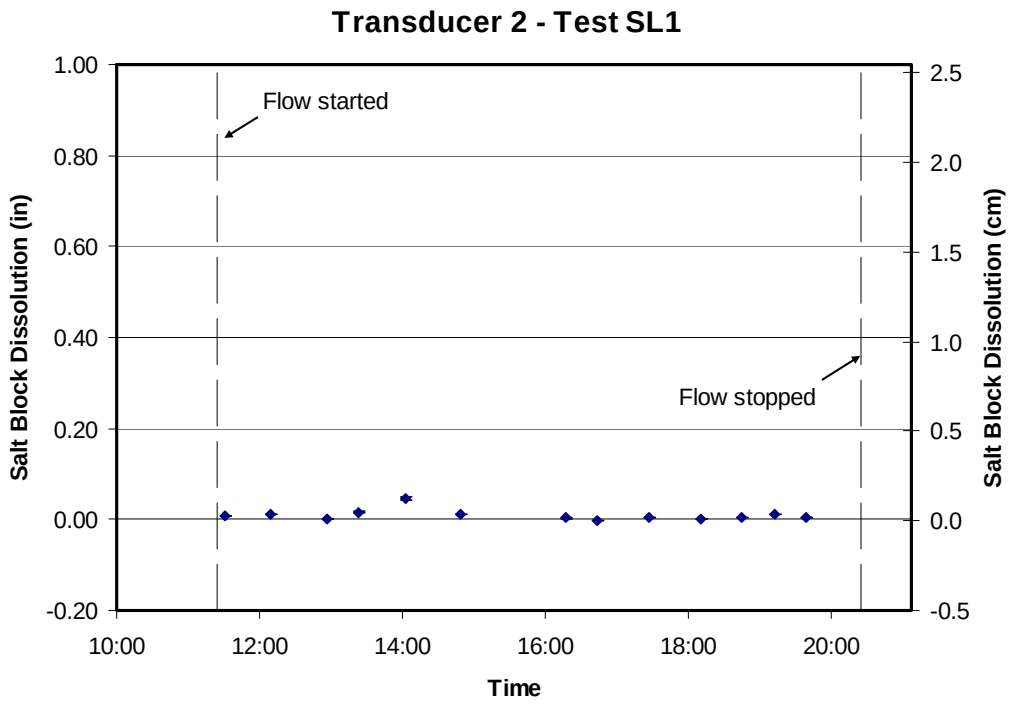

Figure A.2. Ultrasonic data for ultrasonic transducer 2, Test SL1.

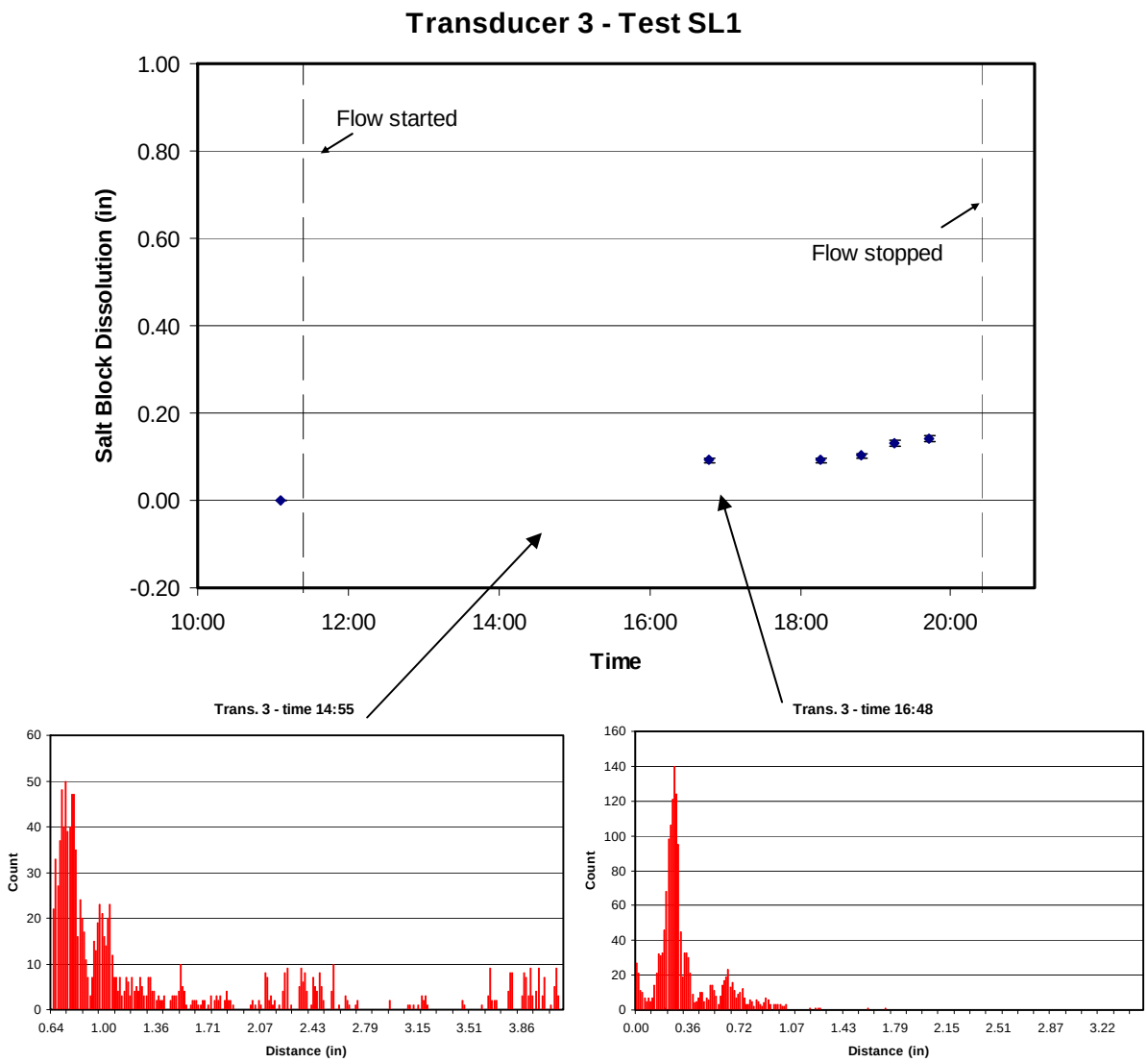

Figure A.3. Ultrasonic data for ultrasonic transducer 3, Test SL1. This plot shows the type of ultrasonic spectra that yielded useful data (right) and data that were not used (left). In this case, the true peak was cut off by the settings needed to eliminate noise sufficiently to acquire a stable signal. Histogram data like these exists for every point in the dissolution vs. time plots but was not all included in this report.

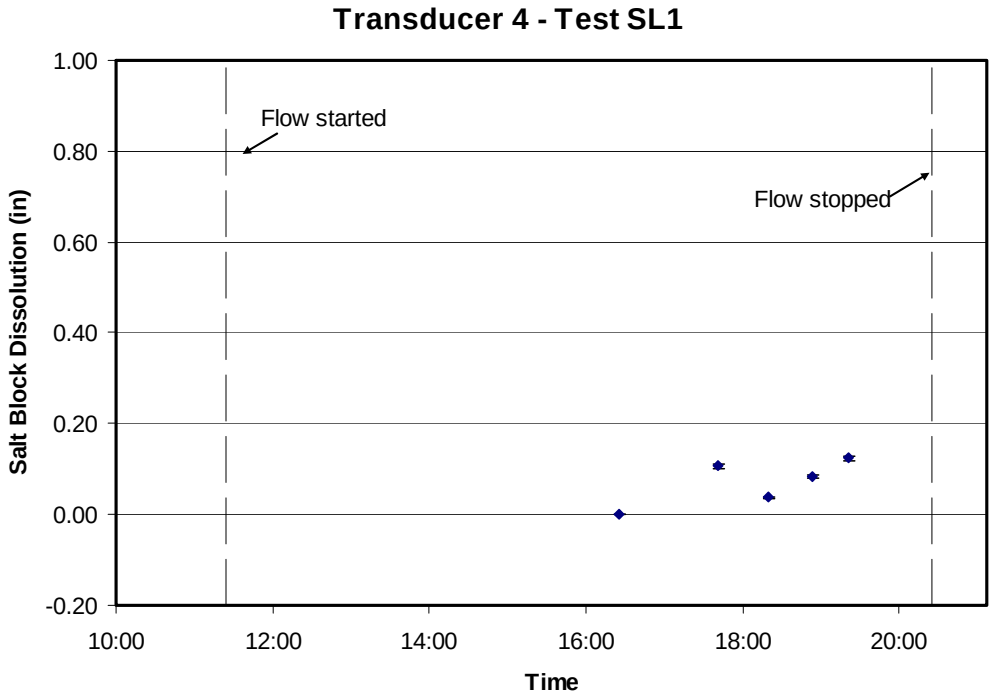

Figure A.4. Ultrasonic data for ultrasonic transducer 4, Test SL1.

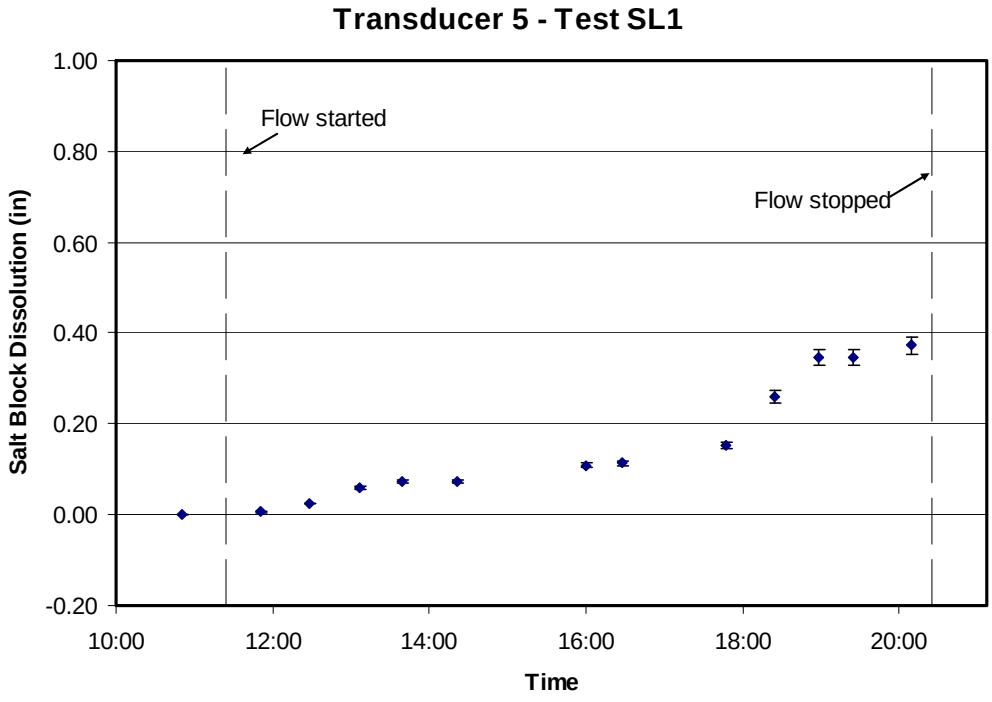

Figure A.5. Ultrasonic data for ultrasonic transducer 5, Test SL1.

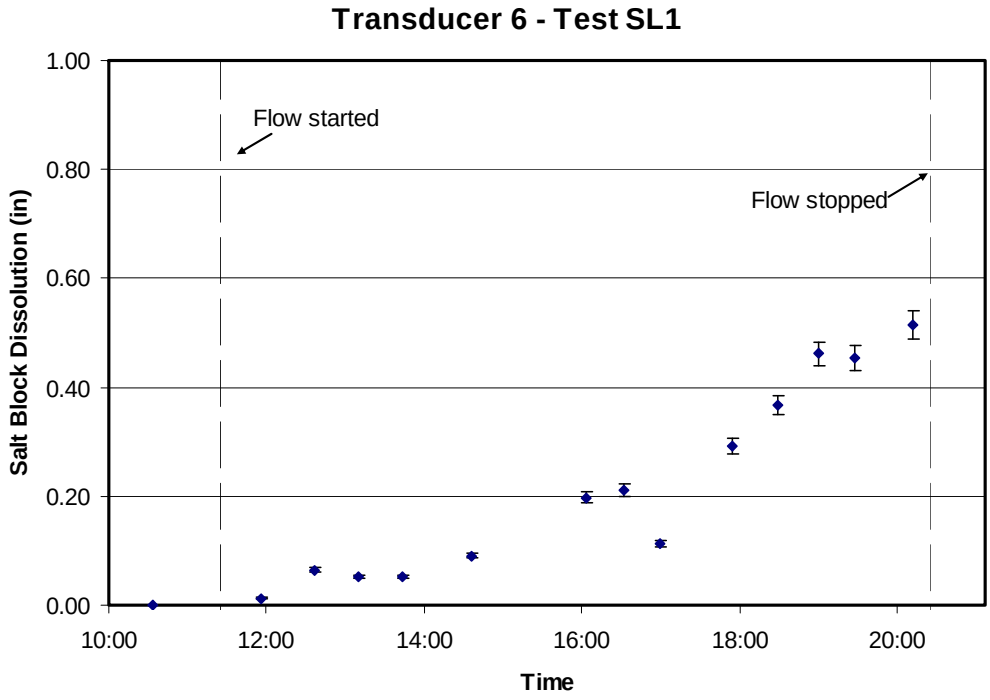

Figure A.6. Ultrasonic data for ultrasonic transducer 6, Test SL1.

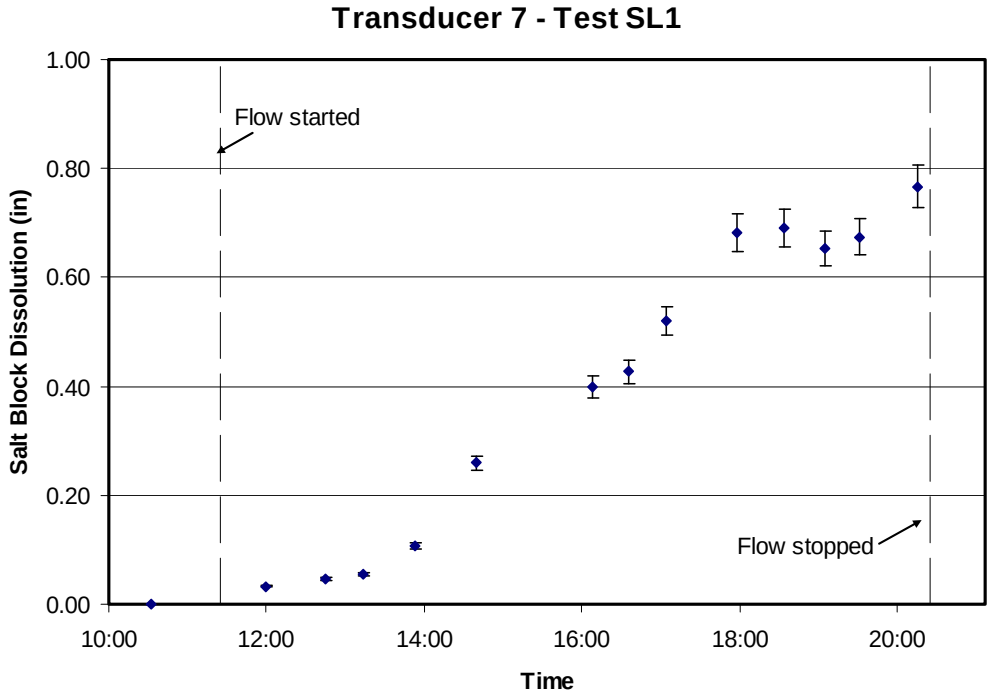

Figure A.7. Ultrasonic data for ultrasonic transducer 7, Test SL1.

Appendix B – Ultrasonic Data for Test RL2

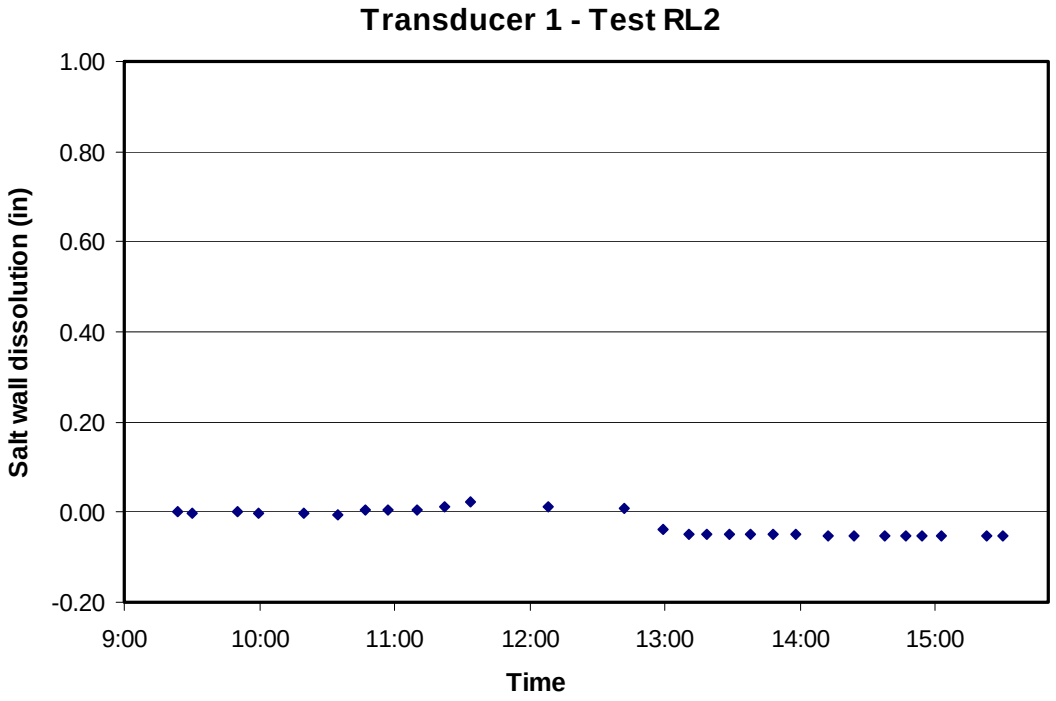

Figure B. 1. Ultrasonic data for ultrasonic transducer 1, Test RL1.

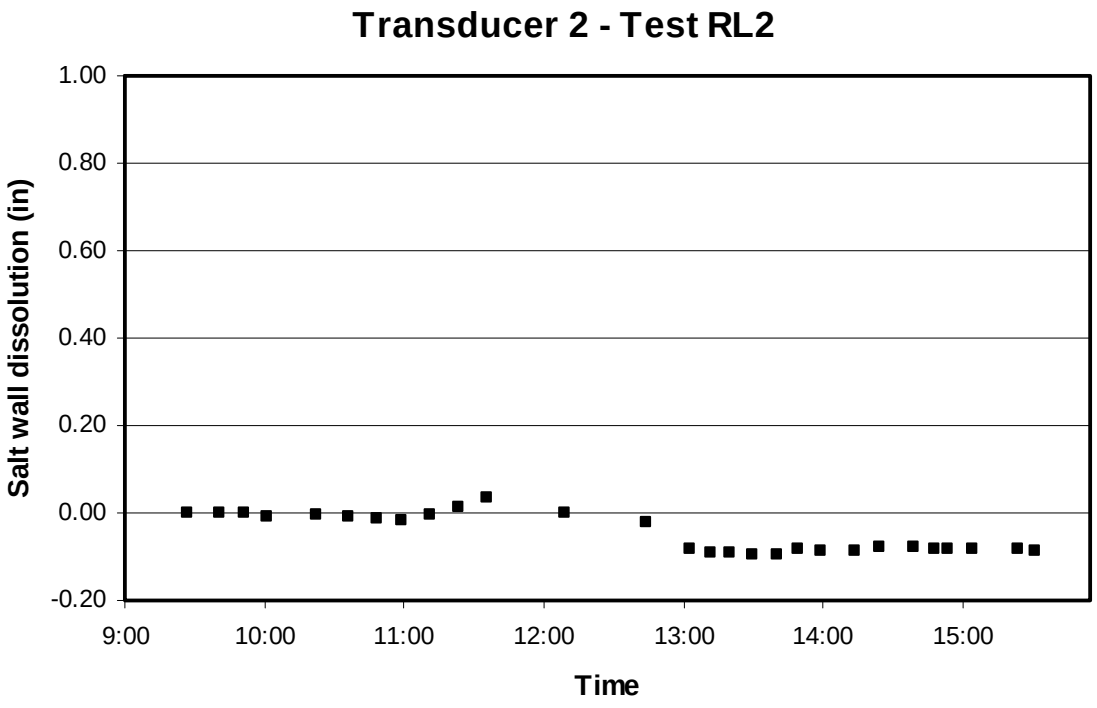

Figure B. 2. Ultrasonic data for ultrasonic transducer 2, Test RL1.

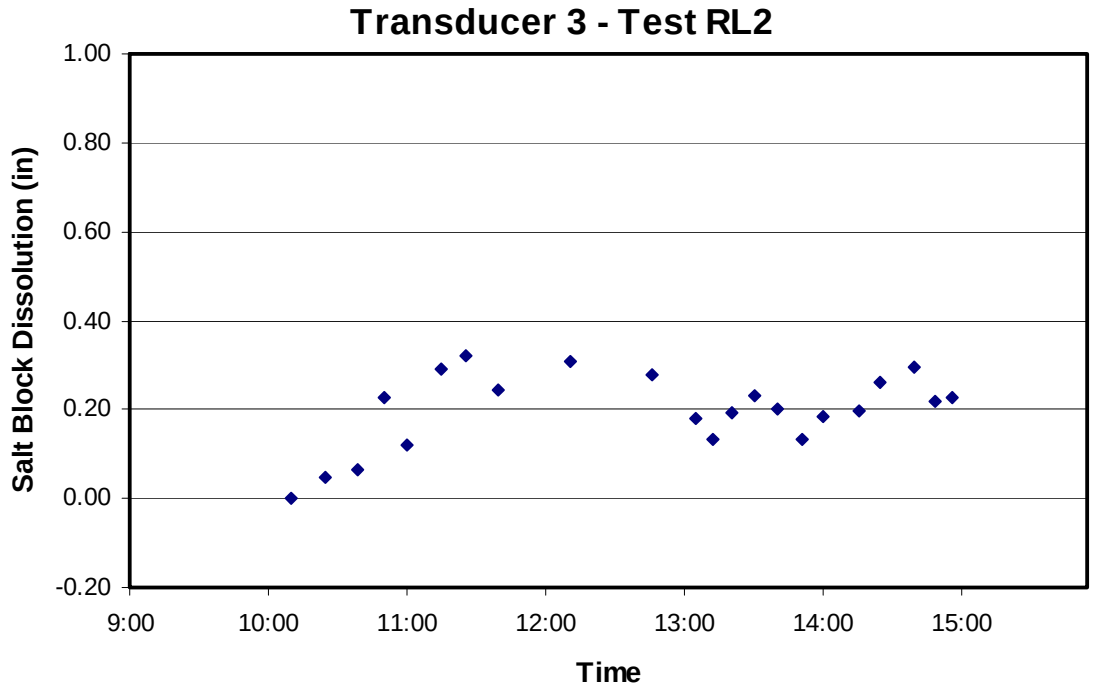

Figure B. 3. Ultrasonic data for ultrasonic transducer 3, Test RL1.

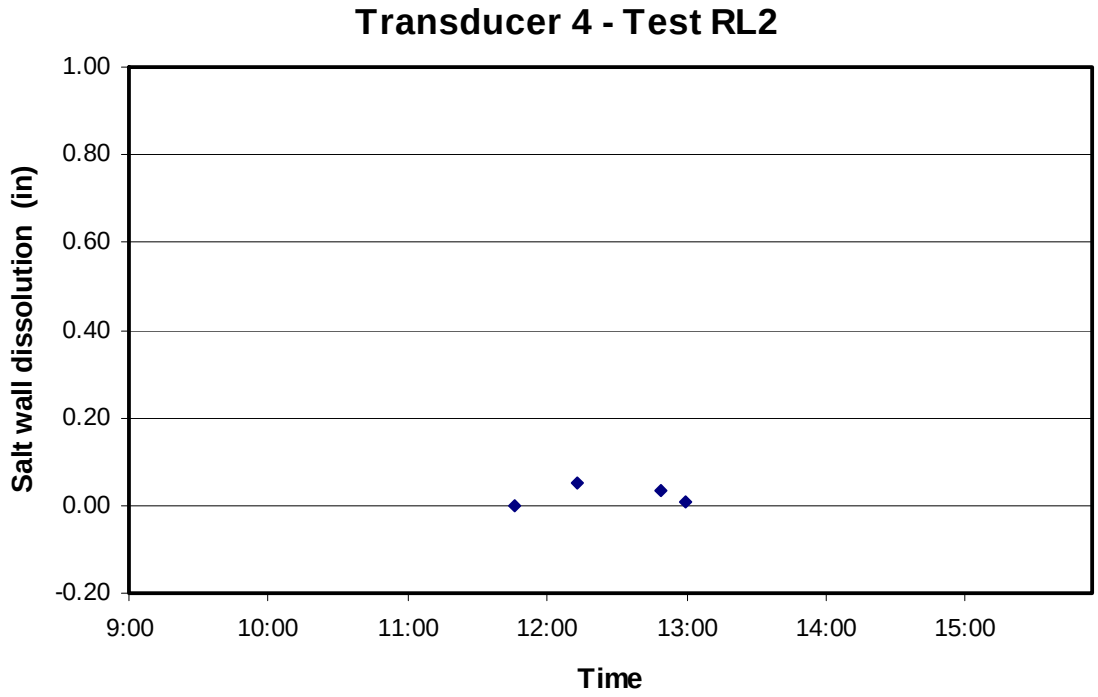

Figure B. 4. Ultrasonic data for ultrasonic transducer 4, Test RL1.

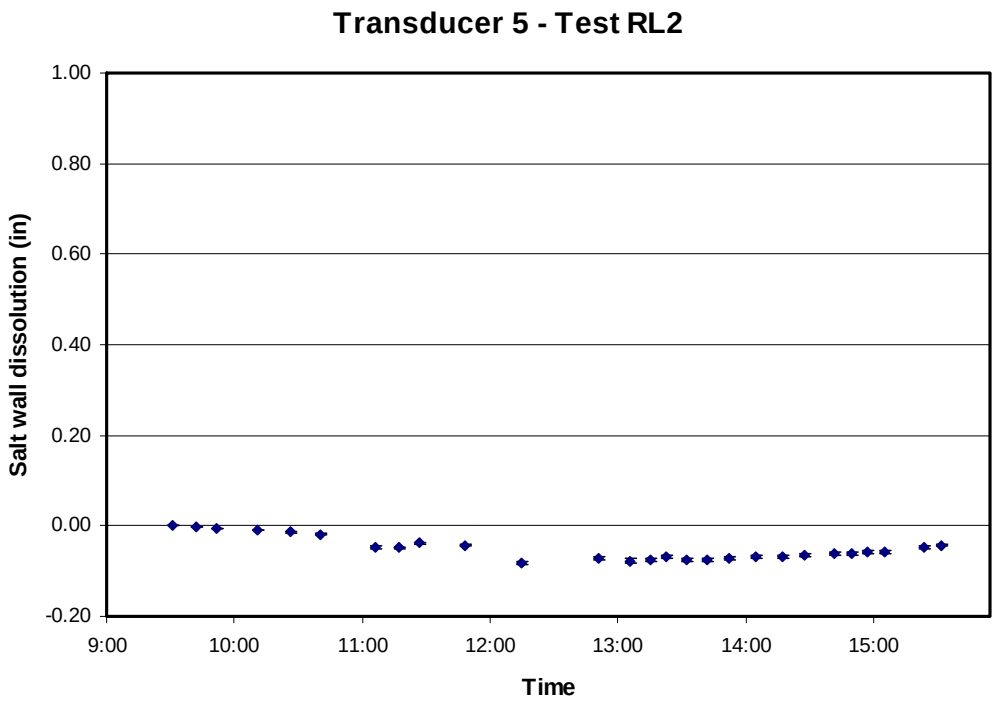

Figure B. 5. Ultrasonic data for ultrasonic transducer 5, Test RL1.

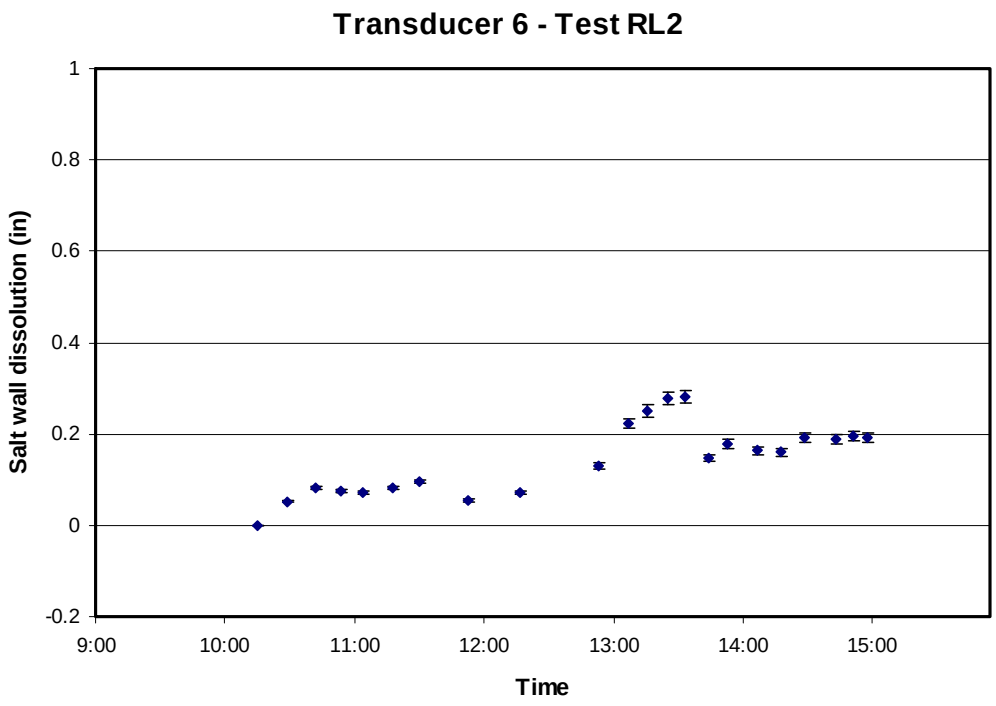

Figure B. 6. Ultrasonic data for ultrasonic transducer 6, Test RL1.

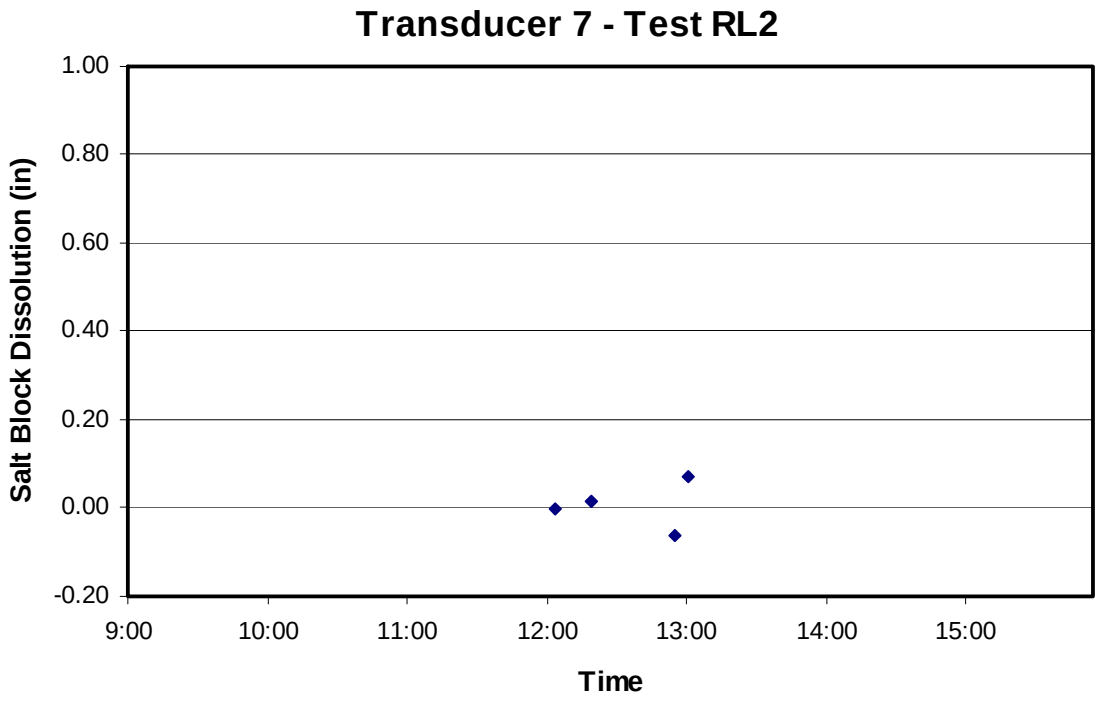

Figure B. 7. Ultrasonic data for ultrasonic transducer 7, Test RL1.

6. References

1. Al-Nassar, Y. N., Al-Jalal, A. M., Khan, M. A., and Al-Kaabi, S. A., 2006, Functional Dependence of Ultrasonic Speed in Water on Salinity and Temperature, NDT.net, 11(6), June.
2. O'Hern, T. J. and Webb, S. W., 2009, SPR Salt Wall Leaching Experiments in Lab-Scale Vessel Completed, Sandia Memo, February 27, 2009.
3. O'Hern, T. J. and Webb, S. W., 2008, Experiment Plan for SPR Salt Wall Leaching Studies in Lab-Scale Vessel, Sandia Memo, December 19, 2008.
4. O'Hern, T. J., Erickson, K. L., Oelfke, J. B., and Lord, D. L., 2008, Results for SPR VOC Transport Studies in Lab-Scale Vessel with Wedged Salt Walls, Sandia Memo, February 29, 2008.
5. Turner, J. S., 1979, *Buoyancy Effects in Fluids* (Cambridge University Press, Cambridge).
6. Webb, S.W., 2008, "Enhancement Factor for the FLUENT Salt Dissolution Model," Milestone Report FY08-2.4(b1), June 30, 2008

7. Distribution

Hardcopies to:

1 MS 0899 Technical Library, 9536 (electronic copy)

Electronic only:

MS 0706	6732	D. J. Borns
MS 0706	6732	D. L. Lord
MS 0706	6732	S. W. Webb
MS 0836	1512	C. J. Bourdon
MS 0836	1512	J. D. Hartenberger
MS 0836	1512	T. J. O'Hern
MS 1146	6763	S. M. Adee

External Distribution (electronic only):
SPR
Darryl James, Texas Tech University